KEM-15 A3: Geological review Study

Risk of Seismicity due to Cooling Effects in Geothermal Systems

172146_REP02_MEZK21_Geol 01 | 16 March 2021

Ministerie van Economische Zaken en Klimaat

Document Control

Document Information

Project Title	Risk of Seismicity due to Cooling Effects in Geothermal Systems
Document Title	KEM-15 A3: Geological review Study
Fugro Project No.	172146 and 1020-169306
Fugro Document No.	172146_REP02_MEZK21_Geol
Issue Number	01
Issue Status	Factual report
Fugro Legal Entity	Fugro France
Issuing Office Address	115 avenue de la Capelado, 34160 Castries France

Client Information

Client	Ministerie van Economische Zaken en Klimaat
Client Address	Bezuidenhoutseweg 732594 AC The Hague
Client Document No.	KEM15

Document History

Issue	Date	Status	Comments on Content	Prepared By	Checked By	Approved By
01	16 March 21	For Review		LB	CD	BW

Project Team

Initials	Name	Role
LB	Lucie BAUDOUY	Geologist
CD	Cédric DUVAIL	Senior Geologist
BW	Beau WHITNEY	Senior Geologist

Contents

1. INTRODUCTION 1
2. UPPER JURASSIC/LOWER CRETACEOUS RESERVOIR: THE DELFT SANDSTONE MEMBER 4
3. SLOCHTEREN FORMATION 6
4. CARBONIFEROUS LIMESTONE (DINANTIAN) 8
5. FAULT TRENDS AND STRESS FIELD 10
5.1 FAULT TRENDS 10
5.2 STRESS FIELD 12
5.2.1 Stress field orientation 12
5.2.2 Stress field variation with depth 13
6. REFERENCES 17
7. APPENDICES – INPUT DATA IN REQUIREMENT LISTS 21

Appendices

A - Upper Jurassic/Lower Cretaceous reservoir: The Delft Sandstone Member

B - Slochteren Formation

C - Carboniferous Limestone (Dinantian)

Figures in the Main Text

Figure 1 : Depth maps of the main geothermal target formations in the Netherlands; doublets targeting these formations are indicated by black dots. 2
Figure 2 : Synthesis of the 2019 geothermal production in the Netherlands 3
Figure 3 : Geographical distribution of the Delft Sandstone Member 5
Figure 4 : Geographical distribution of the Slochteren Formation 7
Figure 5 : Geographical distribution of the Carboniferous Limestone Group 9
Figure 6 : Structural elements map of the Netherlands showing Jurassic and Early Cretaceous basins, highs and platforms (De Jager J., 2007) 11
Figure 7 : Fault pattern at Rotliegend level and flower structures main direction at the base Cretaceous, West Netherlands Basin (De Jager J., 2007) 12
Figure 8 : Stress Map of the Mediterranean and Central Europe 2016 (http://www.world-stress-map.org) 14
Figure 9 : Combination of S_{Hmax} orientation data in both the Limburg Group and the Dinantian. (Osinga S. and Buik N., October 2019) 15
Figure 10 : Cross plot of lithostratigraphic pressure versus depth in the inverted West Netherlands Basin (Verweij et al., 2016) 16

1. Introduction

Fugro was asked to perform a literature review to complete a list of data provided by GFZ German Research Centre for Geosciences in charge of the modelling. These data will be used as entry parameters for the numerical simulations of cooling induced seismicity in the Netherlands.

The same list of data is required for the three hydrothermal reservoirs that will be modelled. The three chosen reservoirs are:

- The Delft Sandstone Member (part of the Schieland Group – Lower Cretaceous). This reservoir is used to simulate a hydrothermal reservoir that sits stratigraphically above the salt;
- The Slochteren Formation (part of the Upper Rotliegend Group – Permian). This reservoir is used to simulate a hydrothermal reservoir that sits stratigraphically below the salt;
- The Carboniferous Limestone (Dinantian). This reservoir is used to simulate a hydrothermal Ultra Deep EGS reservoir.

These reservoirs were chosen based on the current geothermal production in the Netherlands. Figure 1 and Figure 2 show that most of the geothermal energy in the Netherlands is produced in the southwest from Upper-Jurassic and Lower Cretaceous rocks. The Rotliegend reservoir represents installations in Noord-Holland, Overijssel and Flevoland provinces. The Carboniferous reservoir is currently only exploited in the Noord-Limburg area. So far, the produced heat is mainly used to heat commercial greenhouses.

This report is factual. Only a brief description is provided for each reservoir formation. The completed lists of data are provided in appendices in the form of informal internal documents. For ease of reading, the text request from GFZ is left in black. The new text from Fugro is in blue, with *references in gray italics*. As a number of figures have been included from existing publications, we have used a figure numbering system in red.

Note that not all data requested in the list provided by GFZ were found in the literature review.

In order to facilitate the use of these data lists, sources are referred using the pdf naming (all pdf files been provided to the modelling team). This is not the conventional way of referencing but it facilitates the hyperlink between the data and the source. Correlations between pdf names and references are provided in the table in the reference section of this report.

Data values indicated in the lists correspond to “geological” information (from well / core / sample analysis). Values derived from or used in modelling studies are not referenced in the lists.

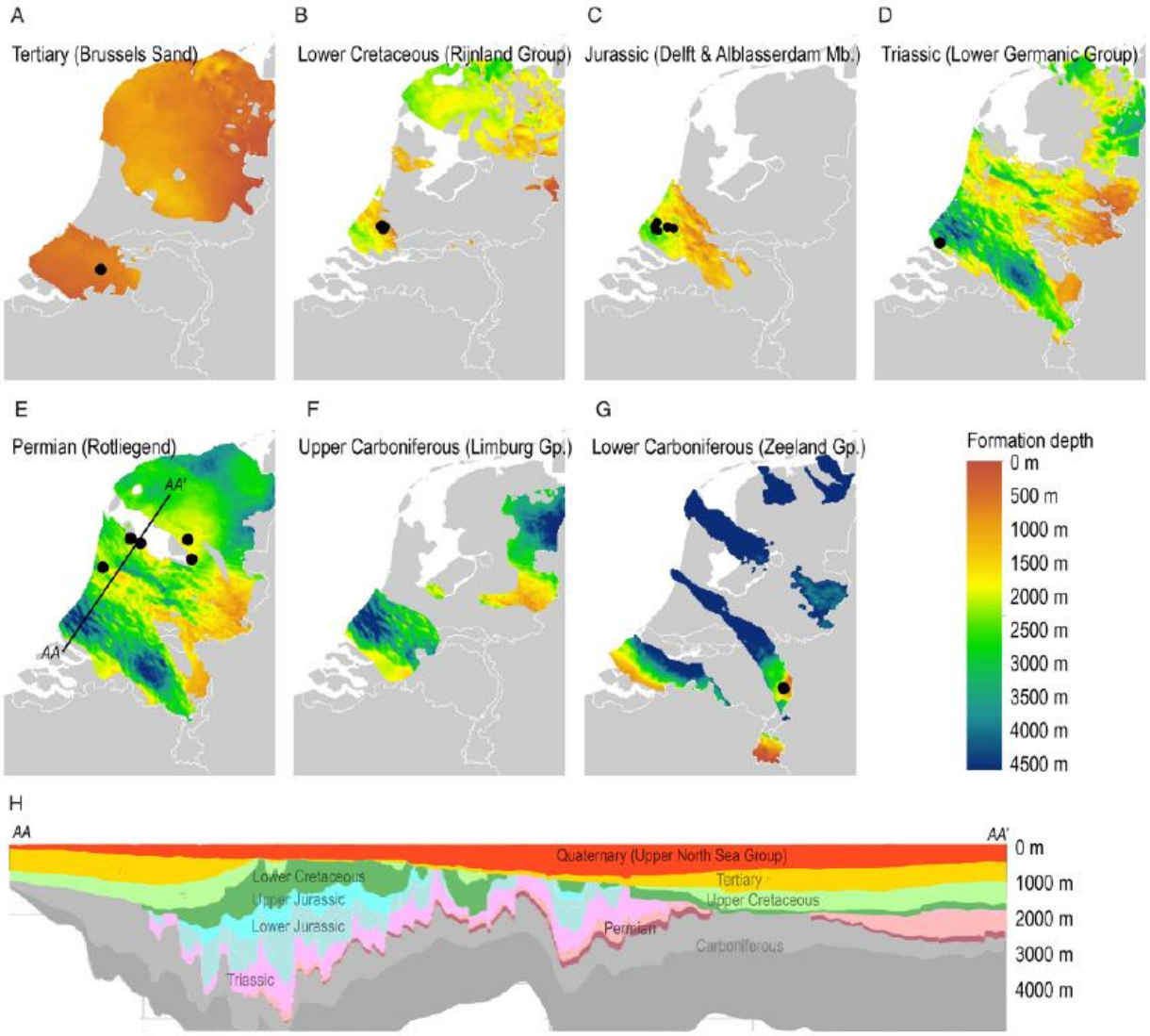

Figure 1: Depth maps of the main geothermal target formations in the Netherlands; doublets targeting these formations are indicated by black dots.

source: Buijze *et al.* (2020)

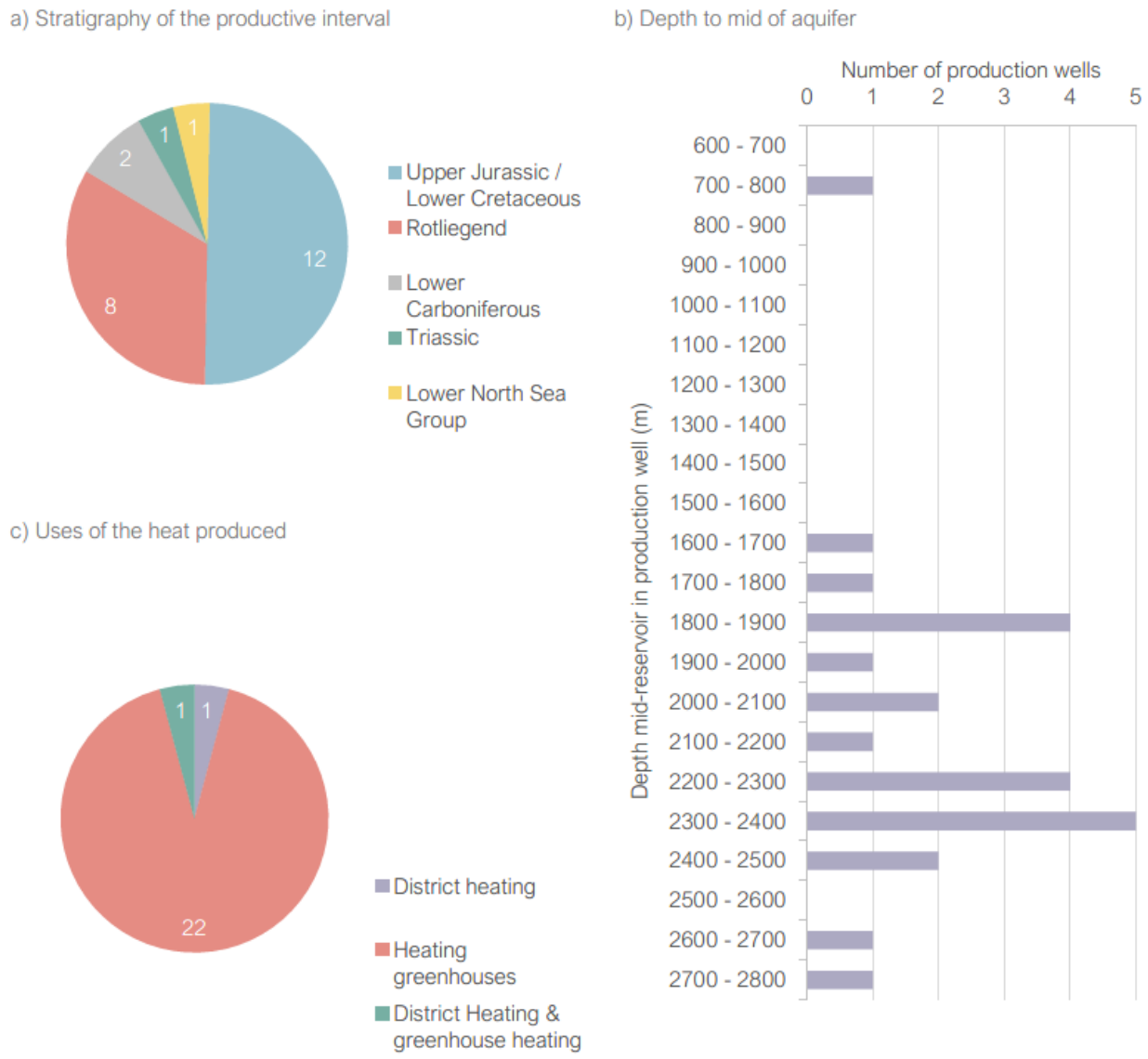

Figure 5.3. a) Stratigraphy of the productive interval, b) Depth to mid of aquifer, c) Uses of the heat produced.

Figure 2 : Synthesis of the 2019 geothermal production in the Netherlands

source: Natural resources and geothermal energy in the Netherlands – Annual review 2019 from the Ministry of Economic Affairs and Climate Policy

2. Upper Jurassic/Lower Cretaceous reservoir: The Delft Sandstone Member

Among the hydrothermal reservoirs above the Permian salt in the Netherlands, we consider the Delft Sandstone Member reservoir. With a Valanginian age (Lower Cretaceous), this stratigraphy interval is part of the Schieland Group.

This sandstone is described in the DINOloket stratigraphic nomenclature (*https://www.dinoloket.nl/en/stratigraphic-nomenclature*) as a "light-grey massive sandstone sequence, fine to coarse-gravelly, fining upward, lignitic". The depositional setting is referred as "Distributary-channels in a lower-coastal-plain setting". With an average thickness of generally less than 145 m at the scale of the whole of the Netherlands, the Delft Sandstone Member conformably overlies the flood-plain deposits of the Alblasserdam Member (used as the bottom layer in the model) and is usually conformably overlain by the organic rich claystones of the Rodenrijs Member (used as the top layer in the model).

The Delft Sandstone Member presents relatively good porosity and permeability values. "Considering an average current depth of the sandstones of 2000–2500 m, these plots suggest a porosity of the Delft Sst of some 8–25% and associated permeability range from several tens of mD up to 3000 mD. Measurements are derived from hydrocarbon wells. So far, well tests from several active geothermal doublets mainly indicate permeability values of entire production intervals of over 1000 mD, which is the higher end of this permeability range." (Willems *et al.*, - 2020).

The underlying "Alblasserdam Mbr is generally considered as a low net-to-gross interval below the Delft Sst Mbr with a low geothermal potential." However, "the sandstone distribution in the Alblasserdam Mbr is poorly understood because most wells only intersect several hundred metres of the top of the Nieuwerkerk Formation. Den Hartog Jager (1996) described the seismic facies of the Alblasserdam section as discontinuous, with low amplitudes. He associated this with rapid lateral facies variation, abundant impermeable shale flow baffles and barriers and lower sandstone content and braided deposits at the base of the member. (…) The limited available core- and well-test data also suggest better aquifer quality of the Delft Sst compared to that of the Alblasserdam Mbr. Mainly the higher temperatures due to the increased depth of up to 3000 m (Duin et al., 2006) still make the Alblasserdam Mbr a considerable potential geothermal target in the WNB, while the increased depth may also influence the permeability and porosity unfavourably." (Willems *et al.*, - 2020).

The overlying Rodenrijs Claystone Member is described as a medium- to dark-grey, silty to sandy lignitic claystones with common laminated or contorted bedding, and lignite/coal beds.

The Delft Sandstone Member is only present is the West Netherlands Basin (South Holland province) (Figure 3) where it is currently used as one of the main reservoir rock for geothermal energy (Figure 1c).

Data collected are from various documents and publications and do not apply to a single identified location.

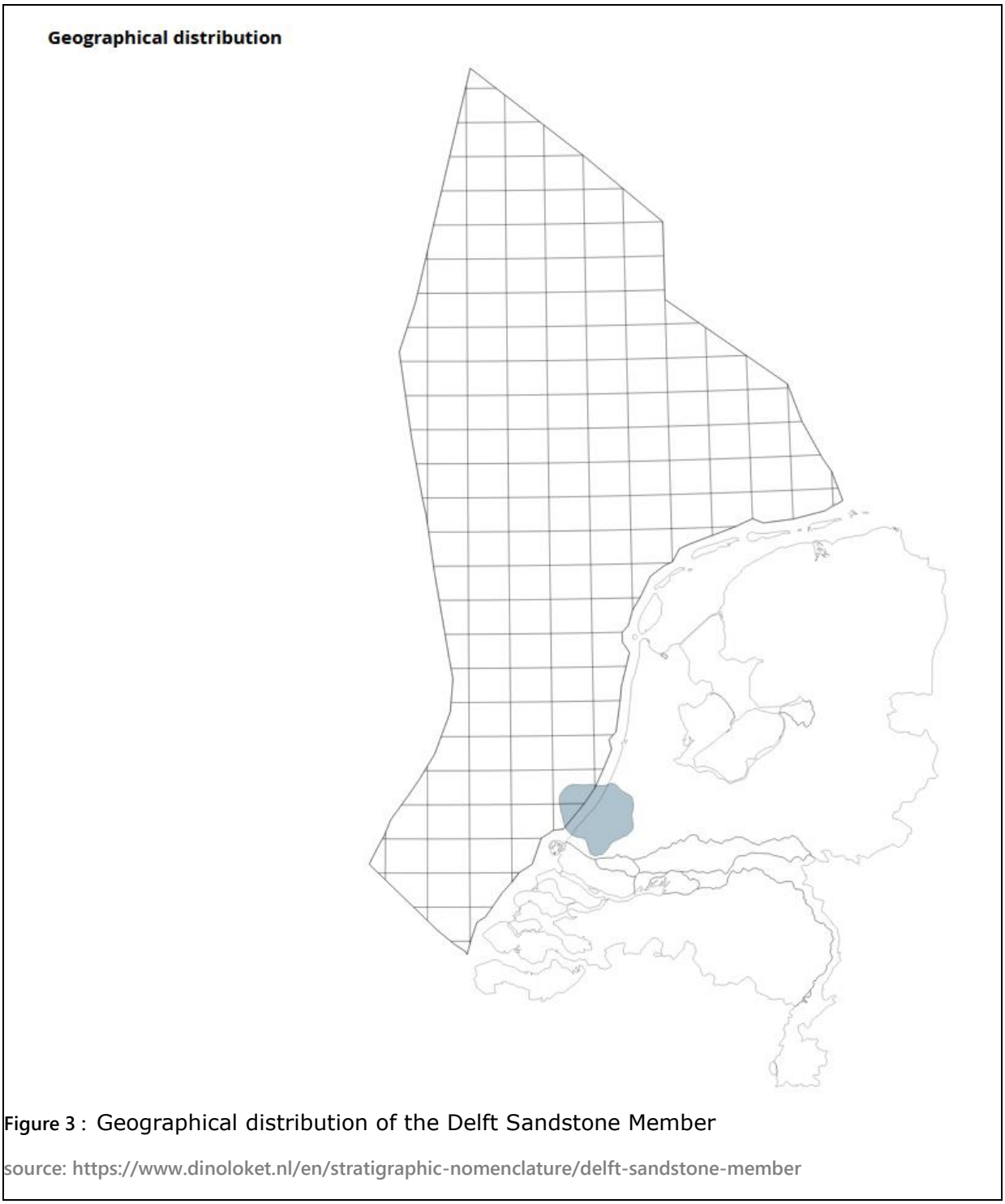

Figure 3 : Geographical distribution of the Delft Sandstone Member

source: https://www.dinoloket.nl/en/stratigraphic-nomenclature/delft-sandstone-member

3. Slochteren Formation

Among the hydrothermal reservoirs below the Permian salt in the Netherlands, we consider the Slochteren Formation reservoir. With a Permian age this stratigraphic interval is part of the Upper Rotliegend Group.

The sandstone intervals form the reservoir. The sandstone is described in the DINOloket stratigraphic nomenclature (https://www.dinoloket.nl/en/stratigraphic-nomenclature) as a "sandstones and conglomerates with subordinate amounts of intercalated (…) silty claystones. The sandstones show a wide range of grain sizes, textures and sedimentary structures. The uppermost tens of metres, immediately below the contact with the Zechstein Group, may show a massive, fluidised or brecciated, intensely cemented character (Mijnlieff et al. 2011, Appendix B)". The depositional setting is referred to as aeolian to fluvial. With a possible reservoir thickness up to 250 m, the Slochteren Formation usually unconformably overlies the Limburg Group (used as the bottom layer in the model). The Slochteren sandstone of the Upper Rotliegend Group forms the Groningen reservoir. Using the Groningen gas field reservoir as analogue, the Zechstein Group could be considered as the top layer for the model.

The whole Limburg Group is described as a group of clastic formations corresponding as an overall regressive deltaic foreland-basin fill. The youngest interval is characterised by (locally coarse-grained) fluvial-plain deposits, some of which exhibit a primary red-bed facies. The group is subdivided in subgroups with variable extent across the Netherlands. Based on the geographical distribution of the various subgroup (see maps in the DINOloket website: https://www.dinoloket.nl/en/stratigraphic-nomenclature), lithology underlaying the Upper Rotliegend Group is predominantly fine-grained deposits.

The Zechstein Group is a relatively complex group in the sense that it is composed by a succession of evaporites and carbonates with some thin intercalations of claystone. The evaporites consist of anhydrite, rock salt and minor amounts of bitter salts, and are locally strongly affected by halokinetic movements. Towards the southern edge of the Southern Permian Basin, siliciclastics gradually replace the evaporites and, to a lesser degree, the carbonates.

The Slochteren Formation is present in most parts of the Netherlands (Figure 4). Few sites currently in activity are exploiting the Upper Rotliegend Group reservoir. These sites are concentrated in Noord-Holland, Overijssel and Flevoland provinces (Figure 1e).

Data collected are from various documents and publications and do not apply to a single identified location but many of the parameter values mostly refer to data provided by the Groningen gas field.

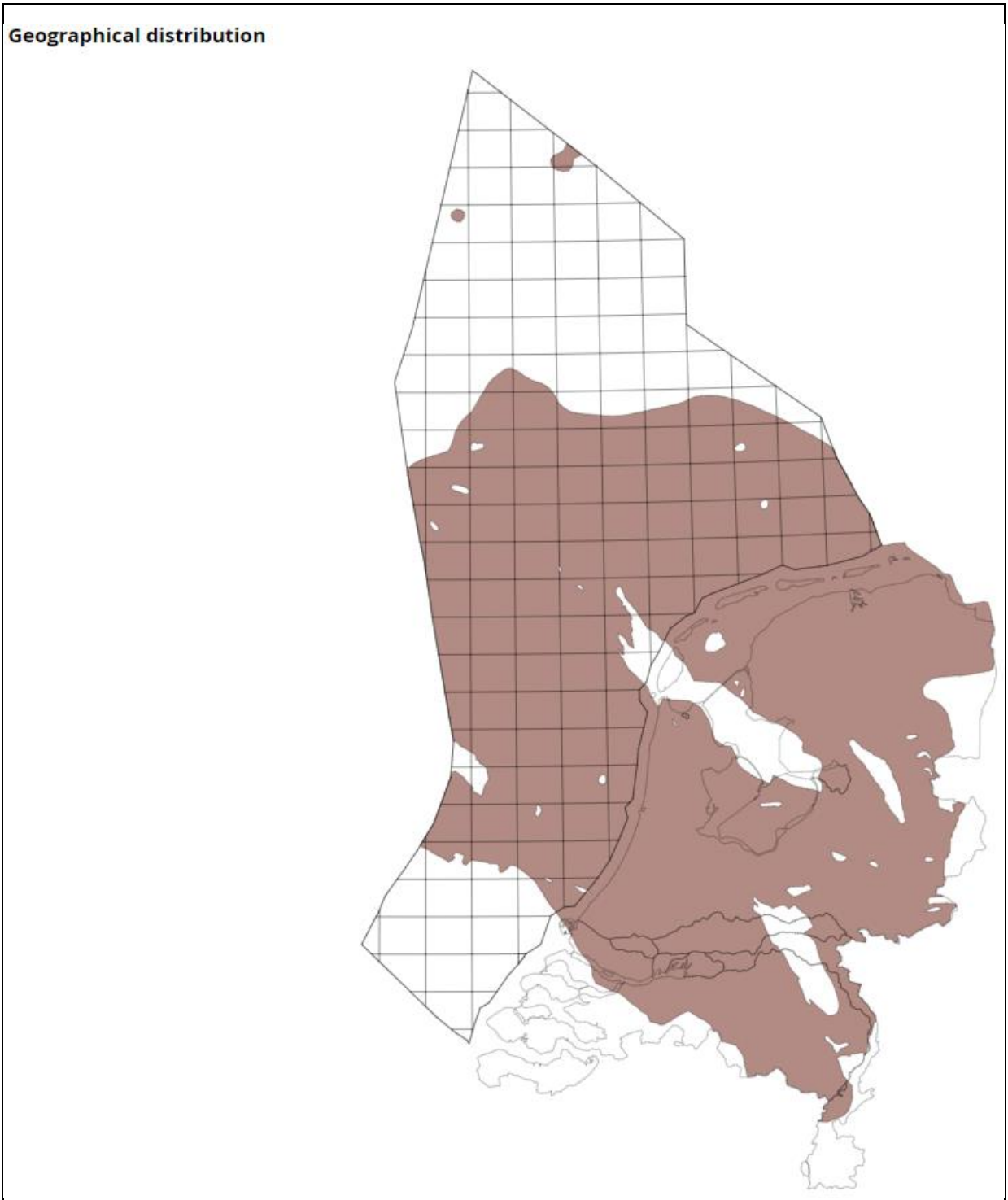

Figure 4 : Geographical distribution of the Slochteren Formation

source: https://www.dinoloket.nl/en/stratigraphic-nomenclature/slochteren-formation

4. Carboniferous Limestone (Dinantian)

The Ultra Deep Geothermal reservoir in the Netherlands (EGS reservoir) refers here to the **Carboniferous Limestone Group** (of Dinantian age). The carbonate rocks of the Lower Carboniferous are known, in the Netherlands, under various names: Dinantian, Carboniferous Limestone Group, Zeeland Formation, Kolenkalk, and sometimes "Kulm".

The Carboniferous Limestone Group is almost present all over the Netherlands. The rocks are currently the target of geothermal exploration and production in the southern part of the Netherlands (Noord-Limburg area - Figure 1g), where they are found at relatively shallow depths (~2 km). In a large part of the Netherlands, however, the rocks are buried very deep (~4-9 km), and are therefore interesting for Ultra Deep Geothermal ("UDG") (*https://www.thermogis.nl/en/dinantian*).

Stratigraphically, the Limburg Group (mostly composed by claystones) sits above the Carboniferous Limestone Group while the Devonian clastic sediments of the Banjaard Group sit below.

The whole Limburg Group is described as a group of clastic formations corresponding as an overall regressive deltaic foreland-basin fill. The oldest interval consists of marine and lacustrine basin-floor fines and turbiditic distal deltaic deposits. Marine influence gradually decreases in time. The group is subdivided into subgroups with variable extent across the Netherlands. The Geul Subgroup, which correspond to the lower part of the Limburg Group comprises cyclic successions of predominantly fine-grained siliciclastic deposits devoid of coal seams.

Unlike the previously mentioned reservoirs corresponding to clastic deposits, the Dinantian reservoir corresponds to carbonate rocks. The rocks have a very low primary permeability but may exhibit karst and/or fault permeability." (*https://www.thermogis.nl/en/dinantian*).

The fact that the reservoir potential is mostly link to both fractures and karsts is also confirmed by others studies: "The carbonates often show low porosities and low permeabilities, but cross-cutting, high-angle fracture systems created some secondary porosity (Vandenberghe et al., 2000). In addition, the Upper Dinantian sediments were subjected to extensive karst processes creating cavernous karst systems with up to metre-scale cavities."
(*dinantian_carbonates_in_the_southern_netherlands_and_northern_belgium.pdf*)

Only few parameters requested in the data list were found during the literature review. Data collected are from various documents and publications and do not apply to a single identified location.

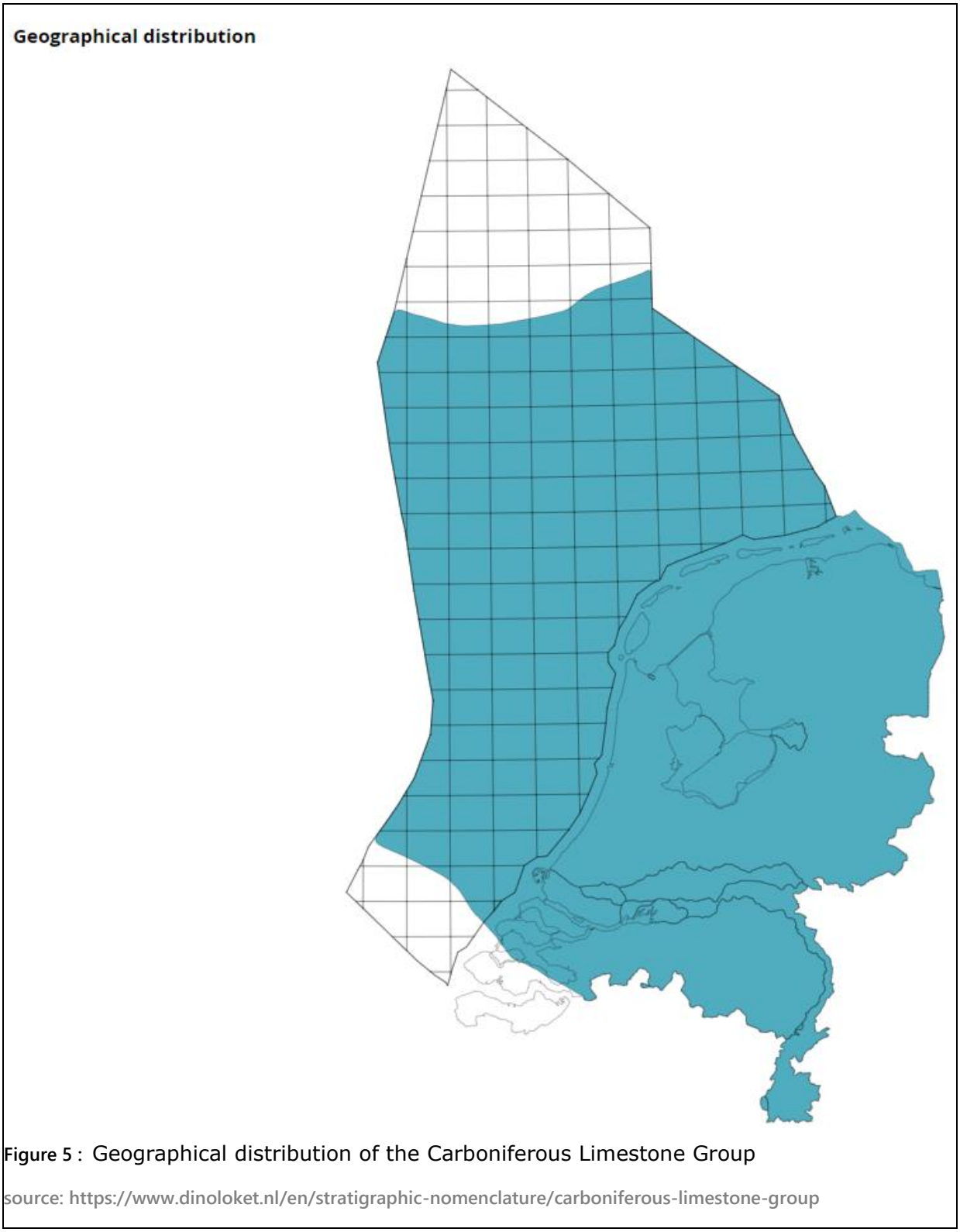

Figure 5 : Geographical distribution of the Carboniferous Limestone Group

source: https://www.dinoloket.nl/en/stratigraphic-nomenclature/carboniferous-limestone-group

5. Fault trends and stress field

5.1 Fault trends

Structural elements directions and fault patterns are relatively homogeneous across the whole onshore part of the Netherlands with a main fault trend varying from NW-SE to NNW-SSE (see maps in Duin *et al.*, 2006). De Jager (2007) makes a general assessment of the fault patterns in the Netherlands where he describes a high degree of fault parallelism despite the many tectonics events. The general structural model is one of repeated reactivation of basement faults (Figure 6) which continue to control the whole Netherlands despite changes in tectonic regime and stress direction. Consequently, most faults have a component of oblique slip.

The fault pattern analysis is focussing on the intervals below and above the Zechstein salt.

At the level of Rotliegend (below the Zechstein salt) De Jager (2007) mentions a rhomboid pattern of intersecting fault with a NW-SE dominant trend inherited from mid-Paleozoic times. The second most common fault trend regionally established during the Early Permian is NE-SW to ENE-WSW oriented. Since both trends were already established prior to the Rotliegend and Zechstein formations, their presence in these younger intervals results from fault reactivation. In the north-east of the Netherlands, the main fault trends in the Rotliegend and Zechstein appear to have rotated slightly to be NNW-SSE and ENE-WSW oriented. Within the West Netherlands Basin, faults affecting the Rotliegend show again an anastomosing pattern dominated by WNW-ESE and NNW-SSE strike-slip faults.

De Jager (2007) mentions that thick salt package has caused faulting above the salt to be decoupled from the basement faulting. However, as many of the salt structures follow main sub-salt fault trends, the salt movements are considered as triggered by basement faulting. For instance, in the north-east of the Netherlands, fault maps at Cretaceous and Tertiary levels shows that both NNW-SSE and ENE-WSW trending faults were reactivated during Tertiary. De Jager (2007) analysis demonstrates that in the West Netherlands Basin, the Late Cretaceous compressional flower-structures were formed through reactivation of both NNW-SSE and WNW-ESE fault trends (Figure 7). What looks like an alignment of continuous flower structures at Cretaceous levels, can be seen to follow different fault trends at Rotliegend level, zigzagging from one to the other. Apparently, none of the pre-existing fault trends was ideally oriented to be preferentially reactivated.

Note that fault patterns mentioned for the West Netherlands Basin (Figure 7) are applicable (among others) to the Delft Sandstone Member reservoir where the formation is located.

Figure 6 : Structural elements map of the Netherlands showing Jurassic and Early Cretaceous basins, highs and platforms (De Jager J., 2007)

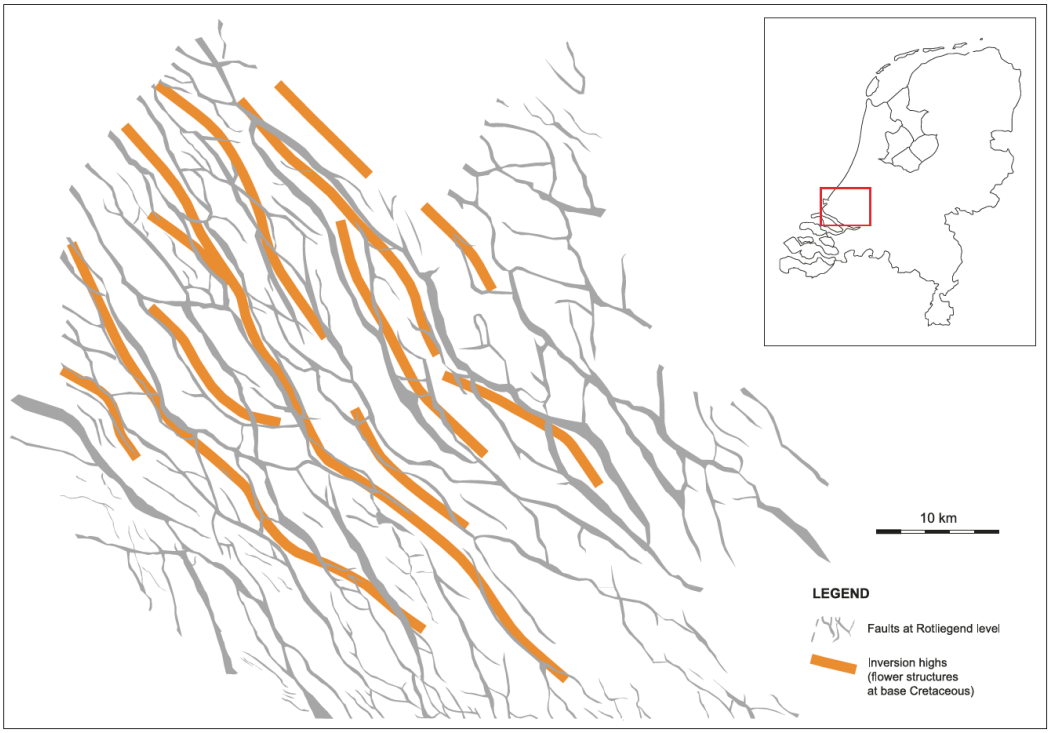

Figure 7 : Fault pattern at Rotliegend level and flower structures main direction at the base Cretaceous, West Netherlands Basin (De Jager J., 2007)

5.2 Stress field

5.2.1 Stress field orientation

A NW-SE direction is frequently indicated for the maximum horizontal stress direction. This direction is precisely the mean direction often accepted for the North Western Europe (Mueller et al., 1992; Zang and Stephansson, 2010), see Figure 8.

The West Netherlands Basin, where the Delft Sandstone Member is described, is tectonically inactive and the stress is extensional with the maximum horizontal stress follow the NW-SE regional stress direction. The stress magnitudes are unknown. Several oil and gas fields targeting the Lower Cretaceous and Upper Jurassic formations are present in the West Netherlands Basin. These fields, although they are located somewhat shallower than the geothermal doublets present in the area, have not led to any induced events over decades of hydrocarbon production, suggesting the stress is not critical (Buijze L, *et al.*, 2020).

The Slochteren is overlain by anhydrites, carbonates and rock salt, which likely have stable stresses due to viscoelastic relaxation (Buijze L, *et al.*, 2020). Seismic events have been observed for gas fields producing from Permian sandstones in the north and west of the Netherlands at a depth of 3 km. These include, among others, the Groningen gas field with >1000 earthquakes with magnitudes up to M_L 3.6. Many of these events occurred after decennia of production, which can be an indication that the state of stress is initially not critical. The formation can be seismogenic, but the stress path and stress changes due to gas depletion are different than those in geothermal systems.

Figure 9 shows the maximum horizontal stress direction in both Limburg and Dinantian levels across the Netherlands. Once again, a mean NW-SE direction can be applied at the scale of the country even when looking at deep to very deep formations (see coherent directions between Figure 8 and Figure 9).

In the province of Limburg, where the deepest formation are currently targeted for geothermal production in the Netherlands, Buijze L, *et al.* (2020) mention that natural seismicity occurs with eight events with $M > 2.2$ within 20 km of the doublets (considering the two Californië sites). Slip tendency analysis indicates that the state of stress on (some) faults including the Tegelen Fault is close to failure (Vörös & Baisch, 2019)

5.2.2 Stress field variation with depth

The principal vertical stress at a certain depth is equivalent to the weight of the overburden (rocks and pore fluids) at that depth. Vertical stress trends will be similar across areas with a simple layer-cake lithostratigraphic sequence and similar burial history.

Verweij *et al.*, 2016 study the spatial variation in vertical stress in the Netherlands. The results of its study show that the vertical stress varies spatially and that the vertical stress gradient is less than the standard gradient (considered standard gradient about 23 MPa/km) in large part of the Netherlands. The largest local deviations from the standard gradient occur in areas with a thick package of low density Cenozoic sediments or in areas with low density salt structures.

Locally, relatively old and more dense stratigraphic units occur at relatively shallow depth on the highs and in strongly inverted parts of basins. In these areas the lithostatic pressure will reach and follow the standard lithostatic pressure gradient already at shallower depths than in other areas. It is the case in the inverted West Netherlands Basin where the plot of Figure 10 shows that at depths of less than 2.5 km the lithostatic gradient is slightly lower than the standard gradient and that it follows the standard gradient at greater depths (Verweij *et al.*, 2016).

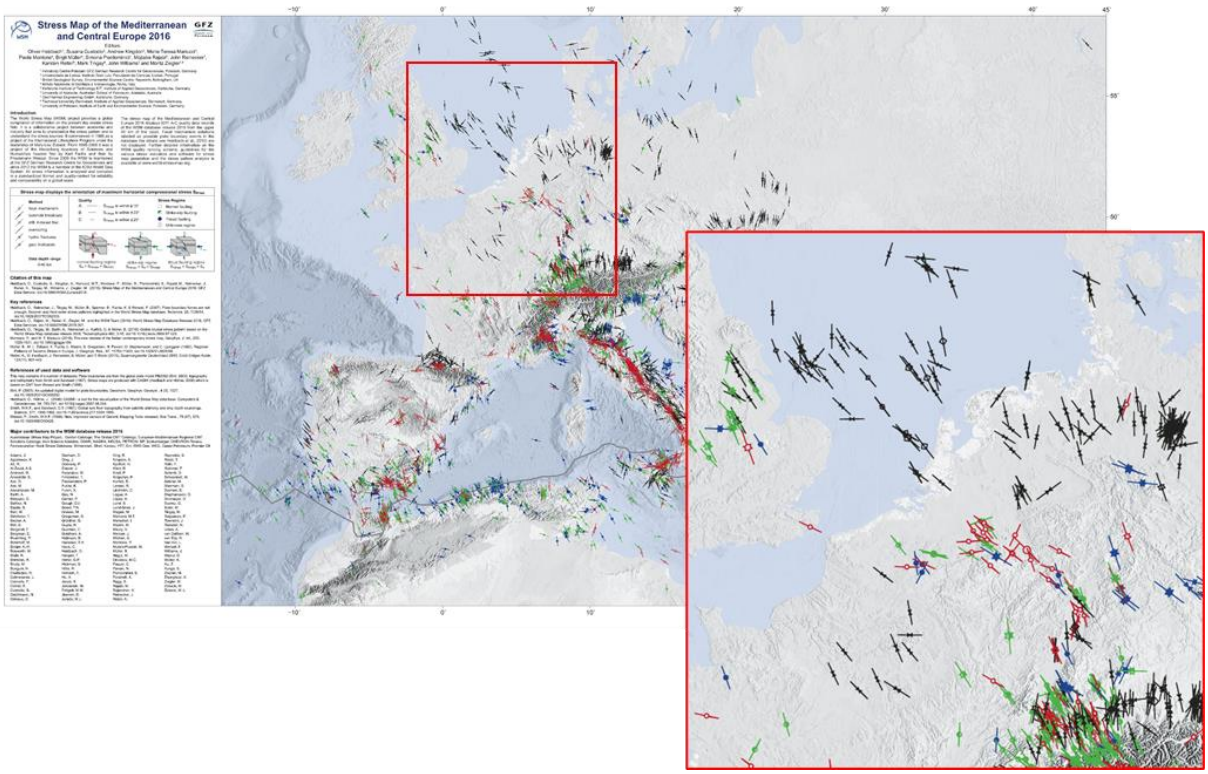

Figure 8 : Stress Map of the Mediterranean and Central Europe 2016 (http://www.world-stress-map.org)

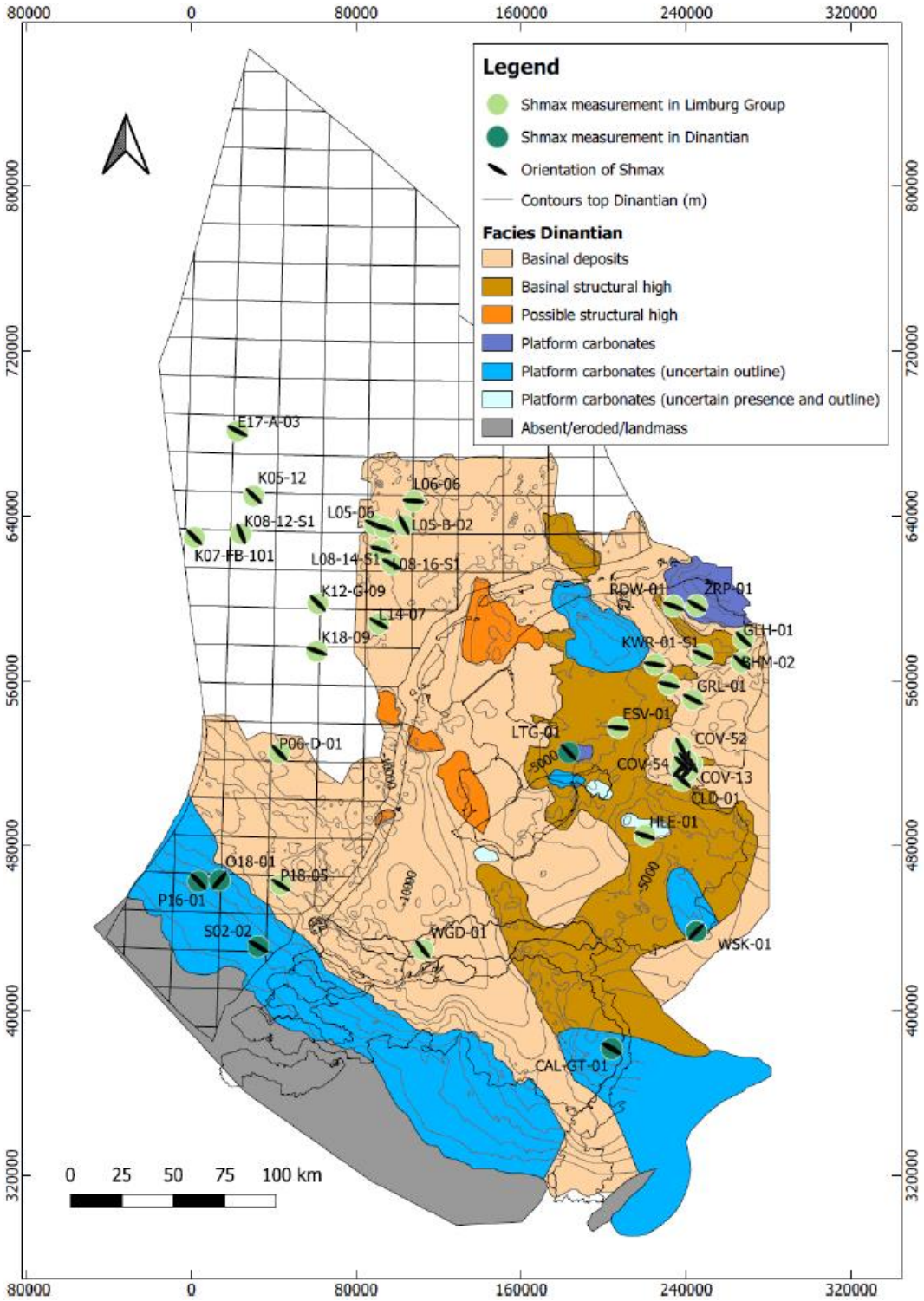

Figure 9 : Combination of S_{Hmax} orientation data in both the Limburg Group and the Dinantian. (Osinga S. and Buik N., October 2019)

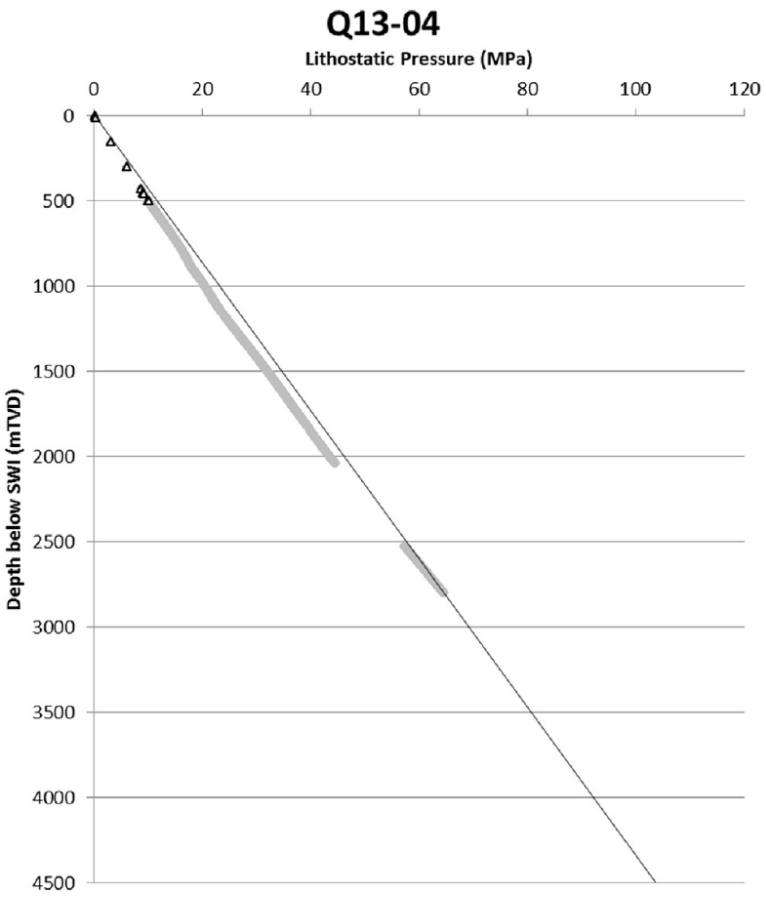

Figure 10 : Cross plot of lithostratigraphic pressure versus depth in the inverted West Netherlands Basin (Verweij et al., 2016)

6. References

List of references used or compiled to complete the KEM15 project geological data requirements for the three considered reservoirs.

.pdf file name	Reference
General_Geothermie folder	
1-s2.0-S167477551630141X-main.pdf	Orlic B., (2016) Geomechanical effects of CO2 storage in depleted gas reservoirs in the Netherlands: Inferences from feasibility studies and comparison with aquifer storage. *Journal of Rock Mechanics and Geotechnical Engineering 8; 846-859*
annual_review_2019_natural_resources_and_geothermal_energy_en_28-9-2020.pdf	Ministry of Economic Affairs and Climate Policy (2019) Natural resources and geothermal energy in the Netherlands – *Annual review 2019 - An overview of exploration, production and subsurface storage*
Buijze_2020_Review_of_induced_seismicity_in_geothermal_systems_worldwide_and_implications_for_geothermal_systems_in_the_netherlands.pdf	Buijze L, et al. (2020). Review of induced seismicity in geothermal systems worldwide and implications for geothermal systems in the Netherlands. *Netherlands Journal of Geosciences, Volume 98, e13*
cornet-Roeckel-Stress profiles Europe.pdf	Cornet F.H., and Röckel T.,: Vertical stress profiles and the significance of "stress decoupling"
Geothermal_energy_use_in_the_Netherlands.pdf	Van Wees J.-D. et al.: Geothermal Energy in the Netherlands: The thermoGIS project… Taking advantage of the oil and gas data and knowledge base. *TNO Presentation*
Geothermal_Wells_Integrity_Final_Report.pdf	Corrosion Review and Materials Selection for Geothermal Wells. (2017) *Report from Wood Group Intetech Ltd– Doc Ref: WGI 5099A*
Introduction_to_the_geothermal_play_and_reservoir_.pdf	Mijnlieff HF. (2020) Introduction to the geothermal play and reservoir geology of the Netherlands. *Netherlands Journal ofGeosciences, Volume 99, e2*
MSc_thesis_Eelco_Mechelse_External.pdf	Mechelse E. (2017) The in-situ stress field in the Netherlands: Regional trends, local deviations and an analysis of the stress regimes in the northeast of the Netherlands *Master of Science Thesis; Delft University of Technology*
Report_6425_Kennisagenda_V_2.1_def_FAULT.pdf	Stegers D.P.M, et al. (2018) Geological study into the geothermal potential near fault zones in the Roer Valley Graben and West Netherlands Basin. *Report from T&A Survey BV. Report number: ODE6425*
tno report_ncp-2a_petrophysics_v150207.pdf	Benedictus T., (2007) Determination of petrophysical properties from well logs of the offshore Terschelling Basin and southern Central North Sea Graben region (NCP-2A) of the Netherlands. *TNO Report*
Verweij et al.2016_vertical stress in the netherlands.pdf	Verweij J.M., Boxem T.A.P. and Nelskamp S. (2016) 3D spatial variation in vertical stress in on- and offshore Netherlands; integration of density log measurements and basin modeling results *Marine and Petroleum Geology 78; 870-882*
Copie de petrofysische analyses-1.xlsx	Petrophysic analyses. F*rom https://www.nlog.nl/en/reservoir-characteristics*
Copie de reservoir eigenschappen-1.xlsx	Reservoir properties. F*rom https://www.nlog.nl/en/reservoir-characteristics*

Copie de Temperature data NL corrected 20180601.xlsx	Temperature data for the Netherlands. *From https://www.nlog.nl/en/temperature-data*
Reservoir_Upper_Jur-Lower_Cret folder	
1-s2.0-S0306261919307469-main.pdf	Willemsa, C.J.L. and Nick H. M. (2019) Towards optimisation of geothermal heat recovery: An example from the West Netherlands Basin. *Applied Energy 247; 582–593*
03GeologicalDevelopment-DeJager.pdf	De Jager J. (2007) Geological development. Geology of the Netherlands *Edited by Th.E. Wong, D.A.J. Batjes & J. de Jager Royal Netherlands Academy of Arts and Sciences, 2007: 5–26*
12054.pdf	Donselaar M.E., et al. (2015) Reservoir Geology and Geothermal Potential of the Delft Sandstone Member in the West Netherlands Basin. *Proceedings World Geothermal Congress 2015 - Melbourne, Australia, 19-25 April 2015*
Cees_Willems_thesis_lower_cretaceous_sands_WNB.pdf	Willems C. (2012) 'Study of the Lower Cretaceous sands in the Van den Bosch Geothermal energy concession'. *Delft University of Technology; TA Report number: AES/TG/12-44*
geology_of_the_upper_jurassic_to_lower_cretaceous_geothermal_aquifers_in_the_west_netherlands_basin_an_overview.pdf	Willems C.J.L. et al. (2020). Geology of the Upper Jurassic to Lower Cretaceous geothermal aquifers in the West Netherlands Basin – an overview. *Netherlands Journal of Geosciences, Volume 99, e1*
MSc_Thesis_Muhammad_Riandy_Eddy_4517482.pdf	Riandy Eddy M. (2017) Prediction of Stress Distribution using 3D Geomechanical Model in De Lier Field, the Netherlands. *Master of Science Thesis; Delft University of Technology*
stimulation_for_geothermal_wells_in_the_netherlands.pdf	de Pater CJ (Hans) and Shaoul JR. (2020) Stimulation for geothermal wells in the Netherlands. *Netherlands Journal of Geosciences, Volume 98, e11*
Folder: Green Well Westland	Information regarding the Honselersdijk project is also provided from the following link: https://www.rvo.nl/subsidies-regelingen/projecten/green-well-westland.
Folder: *c05c_krijt-jura_geothermie_2016-03.zip*	Map showing the Jurassic / Cretaceous geothermal potential repartition in the Netherlands. Data available in various format
Reservoir_Rotliegend folder	
1-s2.0-S0375650516300700-main.pdf	Daniilidis A. et al. (2016) Risk assessment of the Groningen geothermal potential: From seismic to reservoir uncertainty using a discrete parameter analysis. *Geothermics 64; 271-288*
2016.01.04_bia debietverhoging 2-4km_report.pdf	Veldkamp H and Bowem T. (2015). Sector Outlook: Geothermal power increase in the Netherlands by enhancing the capacity. *TNO Report TNO 2015 R11618*
2019JB017366.pdf	Pijnenburg R.P.J., et al. (2019). Inelastic deformation of the Slochteren sandstone: Stress-strain relations and implications for induced seismicity in the Groningen gas field. *Journal of Geophysical Research: Solid Earth, 124, 5254–5282*
148285679.pdf	Doddema L. (2012) The influence of reservoir heterogeneities on geothermal doublet performance. *Default journal*
geothermal_aquifer_performance_assessment_for_direct_heat_production_methodology_and_application_to_rotliegend_aquifers.pdf	Van Wees J-D. et al. (2012) Geothermal aquifer performance assessment for direct heat production – Methodology and application to Rotliegend aquifers. *Netherlands Journal of Geosciences — Geologie en Mijnbouw | 91 – 4 | 651 - 665*
LEAN-D1.03-v2020.02.21-Reservoir-Characterization-Report-public.pdf	Van Wees J-D. et al. (2020) LEAN: Low cost Exploration And deriskiNg of geothermal plays: the Rotliegend demonstrator. Deliverable 1.03: Pre-drill Reservoir Characterization Report
spba-chapter7.pdf	Gast R.E., et al. (2010). Rotliegend. *In: Doornenbal, J.C. and Stevenson, A.G. (editors): PetroleumGeological Atlas of the Southern Permian Basin Area. EAGE Publications b.v. (Houten): 101-121.*

Thesis_Report_Redjosentono.pdf	Redjosentono E.A. (2014) Static aquifer modelling of a Rotliegend Aeolian Sandstone for the Koekoekspolder Geothermal project. *Delft University of Technology. Thesis report: AES/TG/14-03*
VeldkampetalWGC2015Permian_rotliegend_architecture_koekoekspolder.pdf	Veldkamp J.G. et al (2015) Permian Rotliegend Reservoir Architecture of the Dutch Koekoekspolder Geothermal Doublet. *Proceedings World Geothermal Congress 2015 - Melbourne, Australia, 19-25 April 2015*
Folder: *c05a_slochteren_geothermie_2016-03.zip*	Map showing the Slochteren geothermal potential repartition in the Netherlands. Data available in various format
Reservoir_Dinantian folder	
1-s2.0-S187661021401755X-main.pdf	Loveless S. et al. (2014) Mapping the geothermal potential of fault zones in the Belgium-Netherlands border region. *European Geosciences Union General Assembly 2014, EGU 2014; Energy Procedia 59 (2014) 351 – 358*
Verweij-NJG-91-4-4_2012.pdf	Verweij J.M. et al. (2012) Pressure and fluid dynamic characterisation of the Dutch subsurface. *Netherlands Journal of Geosciences — Geologie en Mijnbouw | 91 – 4 | 465 - 490*
dinantian_carbonates_in_the_southern_netherlands_and_northern_belgium.pdf *dinantian_carbonates_in_the_southern_netherlands_and_northern_belgium_supp_materials.xlsx*	Reijmer J.J.G. et al (2017) Seismic stratigraphy of Dinantian carbonates in the southernNetherlands and northern Belgium. *Netherlands Journal of Geosciences — Geologie en Mijnbouw |96 – 4 | 353–379*
200906_EAGE_Luttelgeest.pdf *200906_EAGE_Luttelgeest_Abstract.txt*	Van Hulten F.F.N. and Poty Edouard. (2009). Dinantian Reefs underneath the Netherlands. *European Association of Geoscientists & Engineers 71st Conference & Exhibition– June 8th – 11th 2009 – Amsterdam, the Netherlands*
ndx_terheege.pdf	Ter Heege J. and Osinga S. (2020) Flow and Performance of Geothermal Doublets in Deep Dinantian Carbonates of The Netherlands. *Adapted from oral presentation given at 2018 AAPG European Region, Geothermal Cross Over Technology Workshop, Part II, Utrecht, TheNetherlands, April 17-18, 2018. Search and Discovery Article #80720 (2020)*
382.pdf	Heijnen L. et al. (2019) Ultra Deep Geothermal program in the Netherlands. *European Geothermal Congress 2019Den Haag, The Netherlands, 11-14 June 2019*
Voet_et_al_2020_fracture_characteristics_Belgium.pdf	van der Voet E, et al. (2020). Fracture characteristics of Lower Carboniferous carbonates in northern Belgium based on FMI log analyses. *Netherlands Journal of Geosciences, Volume 99, e8*
Msc_thesis_Dominique_Reith_TU_Delft.pdf	Reith D.F.H (2017) Dynamic simulation of a geothermal reservoir – Case study of the Dinantian carbonates in the Californië geothermal wells, Limburg, NL. *Delft University of Technology. Thesis report*
NLOG_GS_PUB_1519_SCAN_Fracture_Characterization_of_the_Dinantian_Carbonates_in_the_Dutch_Subsurface.pdf	van Leverink D. and Geel K. (November 2019) Fracture characterization of the Dinantian carbonates in the Dutch subsurface. *Report by SCAN*
scan_dinantien_petrophysical_report_of_the_dinantian_carbonates_in_the_dutch_subsurface_0.pdf	Carlson T. (April 2019) Petrophysical Report of the Dinantian Carbonates in the Dutch Subsurfaceacies analysis and diagenetic evolution of the Dinantian carbonates in the Dutch subsurface. *Report by SCAN*
WP2.1.1_WP2.1.2_Seismic_interpretation_and_depth_conversion_report.pdf	ten Veen J. et al. (September 2019) Seismic Interpretation and Depth Conversion of the Dinantian carbonates in the Dutch subsurface. *Report by SCAN*
scan_dinantian_facies_analysis_and_diagenetic_evolution_of_the_dinantian_carbonates_in_the_dutch_subsurface.pdf	Mozafari M. et al. (September 2019) Facies analysis and diagenetic evolution of the Dinantian carbonates in the Dutch subsurface. *Report by SCAN*

scan_dinantian_facies_analysis_and_diagenetic_evolution.pdf *LOG_scan_dinantian_facies_analysis_and_diagenetic_evolution_-_appendix_c.pdf*	Mozafari M. et al. (September 2019) Facies analysis and diagenetic evolution of the Dinantian carbonates in the Dutch subsurface: overview and synthesis. *Report by SCAN*
scan_dinantian_estimating_geothermal_power_of_ultra-deep_dinantian_carbonates_in_the_dutch_subsurface.pdf	Bruijnen P. (September 2019) Estimating geothermal power of ultra-deep Dinantian carbonates in the Dutch subsurface. *Report by SCAN*
scan_dinantian_2.1.4_non-seismic_-_review_em_methods.pdf	van Leeuwen W. (December 2019) Electromagnetic geothermal exploration in the Netherlands - review of the CSEM and MT methods. *Report by SCAN*
scan_dinantian_stress_field_characterization_dinantian_carbonates_report.pdf	Osinga S. and Buik N. (October 2019) Stress field characterization in the Dinantian carbonates in the Dutch subsurface. *Report by SCAN*
SCAN Dinantian Temperature modelling Dutch subsurface at depth Dinantian report.pdf	Veldkamp J.G. and Hegen D. (April 2020) Temperature modelling of the Dutch subsurface at the depth of the Dinantian. *Report by SCAN*
scan_survey_gebied_c_voor_publicatie_20191030.pdf	ter BorghM. and Mijnlieff. H. (October 2019) Geological evaluation for the seismic acquisition programme for SCAN area C (Nijmegen – Haarlem). *Report by SCAN*
scan_survey_gebied_ab_voor_publicatie_20191030.pdf	van Lochem H. et al. (October 2019) Geological evaluation for the seismic acquisition programme for SCAN areas A (Noord-Gelderland and Zuidoost Flevoland) and B (Achterhoek and Zuid-Twente). *Report by SCAN*
interpretation_coverage_top_Dinantian.pdf	Map: Interpretation coverage top Dinantien Source: https://www.nlog.nl/en/scan-2d-seismic-interpretation-and-depth-conversion-dinantian
base_dinantien_tvd_si_welltied.pdf	Map: Depth Base Dinantien Source: https://www.nlog.nl/en/scan-2d-seismic-interpretation-and-depth-conversion-dinantian
top_dinantien_tvd_si_welltied.pdf	Map: Depth Top Dinantien (well tied) Source: https://www.nlog.nl/en/scan-2d-seismic-interpretation-and-depth-conversion-dinantian
Folder: *SCAN_DINANTIAN 2.1.3 Burial and structuration*	Bouroullec R. et al. (September 2019) Burial and Structural Analysis of the Dinantian Carbonates in the Dutch Subsurface. *Report by SCAN* *+ cross-sections files*

Additional references:

Duin E.J.T., Doornenbal J.C., Rijkers R.H.B., Verbeek J.W. and WONG Th.E. (2006) Subsurface structure of the Netherlands – results of recent onshore and offshore mapping. Netherlands Journal of Geosciences – Geologie en Mijnbouw, 85-4, 245-276

7. Appendices – Input data in requirement lists

A - Upper Jurassic/Lower Cretaceous reservoir: The Delft Sandstone Member

B - Slochteren Formation

C - Carboniferous Limestone (Dinantian)

Note that input data provided in appendices are in the form of informal internal documents.

Appendix A

Upper Jurassic/Lower Cretaceous reservoir: The Delft Sandstone Member

t

GFZ Helmholtz Centre Potsdam

[Appendix Heading 2]
[Appendix Heading 3]

[Enter text/content]

HELMHOLTZ CENTRE POTSDAM
GFZ GERMAN RESEARCH CENTRE FOR GEOSCIENCES

Dr. Hannes Hofmann

Section 4.8

Telegrafenberg

hannes.hofmann@gfz-potsdam.de

Telephone: +49 (0)331 288-28739

Potsdam, 07 September 2020

Data requirements for KEM-15 ("Cooling induced seismicity")

This document contains a list of data reqired to perform the numerical simulations of cooling induced seismicity using the Finite Element Code GOLEM. The model is based on the published and history matched GOLEM model of Groß Schönebeck Enhanced Geothermal System. Based on this model up to 5 generic and specific models will be built:

1 generic hydrothermal model (shallower, no stimulated fractures)
1 generic EGS model (deeper, with stimulated fractures)
1 specific hydrothermal reservoir above salt in the Netherlands
1 specific hydrothermal reservoir below salt in the Netherlands
1 specific deep EGS reservoir in the Netherlands

This document concerns the hydrothermal reservoir above the Permian salt in the Netherlands. The considered reservoir formation is the **Delft Sandstone Member** which is part of the Schieland Group.
The Rodenrijs Claystone Member forms the top layer.
The Alblasserdam Member forms the bottom layer.

The Delft Sandstone Member is only present is the West Netherlands Basin (South Holland province - Figure 2) where it is currently used as one of the main reservoir rock for geothermal energy. Many of the parameter values added into the following tables refer to data collected from various documents and publications and do not apply to a single identified location.

Parameter values indicated in this document correspond to "geological" information (from well / core / sample analysis). Values derived from or used in modelling studies are not indicated in here.

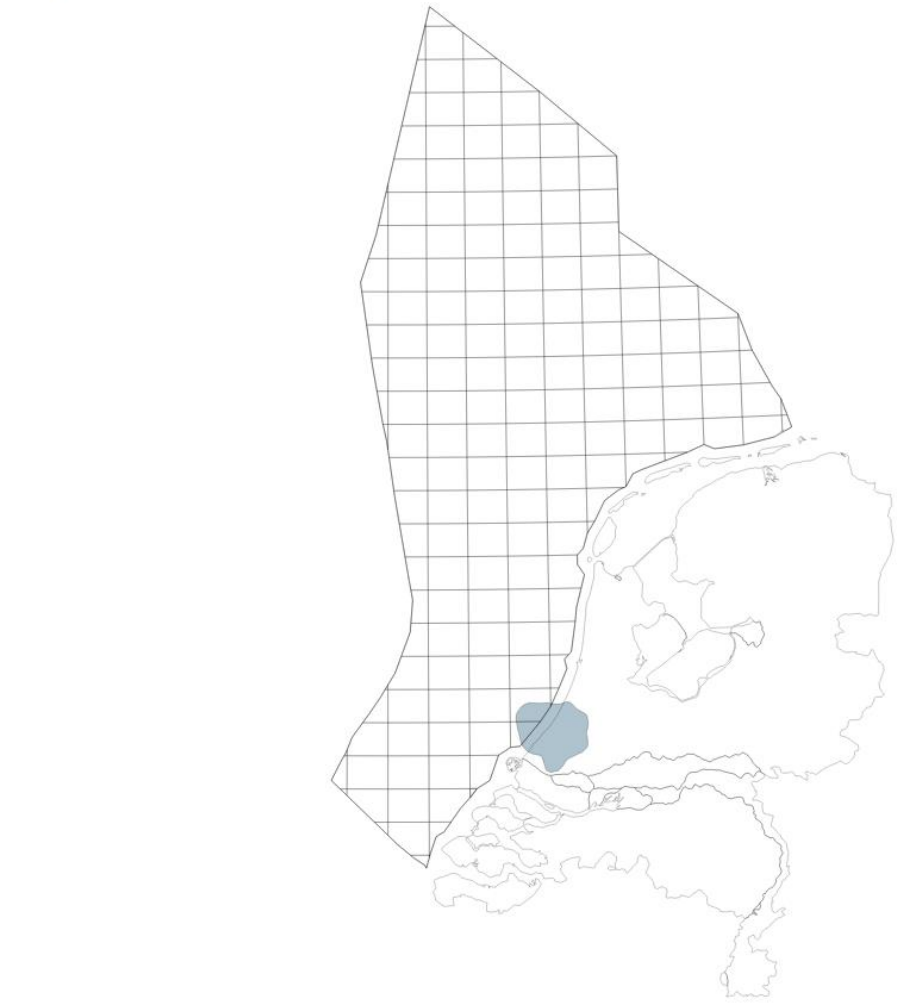

Figure 1 : Geographical distribution of the Delft Sandstone Member

source: https://www.dinoloket.nl/en/stratigraphic-nomenclature/delft-sandstone-member

For each of these models the parameter list below is required.

1. Geological models (geometry)

For the specific reservoir models a GOCAD (*.gp) file of the reservoir geometry would be best. Alternatively, the individual faults, surfaces and well paths may be provided as point data (X, Y, Z). For the generic models the table below is enough.

Property (unit)	Mean value	Min. value	Max. value	Source
Reservoir unit top (m)		2000	2300	"see *Figure 3*" + description in the text *Source: Donselaar et al (2015) - 12054.pdf*
	2300	1855	2480	"see Figure 4" + description in the text *Source: Willems and Nick (2019) - 1-s2.0-*

				S0306261919307469-main.pdf
Reservoir unit thickness (m)		56	112	"see *Figure 3*" + description in the text *Source:* Donselaar et al (2015) - 12054.pdf
Top layer thickness (m) = Rodenrijs Claystone Member		10 60	130 120	"see *Figure 3*" + description in the text *Source:* Donselaar et al (2015) - 12054.pdf "see *Figure 5*" *source: Willems (2012) - Cees_Willems_thesis_lower_cretaceous_sands_WNB.pdf*
Bottom layer thickness (m) = Alblasserdam Member		>300	>500	"see *Figure 3*" + description in the text *Source: Donselaar et al (2015) - 12054.pdf*
# of fault sets	2			"see *Figure 6*" *Source: de Jager (2007) - 03GeologicalDevelopment-DeJager.pdf*
Fault set strike (° from N)	N130°E & N150°E			"see *Figure 6*" *Source: de Jager (2007) - 03GeologicalDevelopment-DeJager.pdf*
Fault set dip (° from hor.)	80°			Strike-slip faults are usually subvertical faults
Fault set dip direction (° from N)	N040°E - N220°E & N060°E - N240°E			"see *Figure 6*" *Source: de Jager (2007) - 03GeologicalDevelopment-DeJager.pdf*
Fault length (m)	25 000	10 000	>60 000	Only main faults are represented here. "see *Figure 6*" *Source: de Jager (2007) - 03GeologicalDevelopment-DeJager.pdf*
Fault spacing (m)	5000m for the main faults			"see *Figure 6*" *Source: de Jager (2007) - 03GeologicalDevelopment-DeJager.pdf*
Units intersected by fault	All considered units (reservoir, top and bottom)			

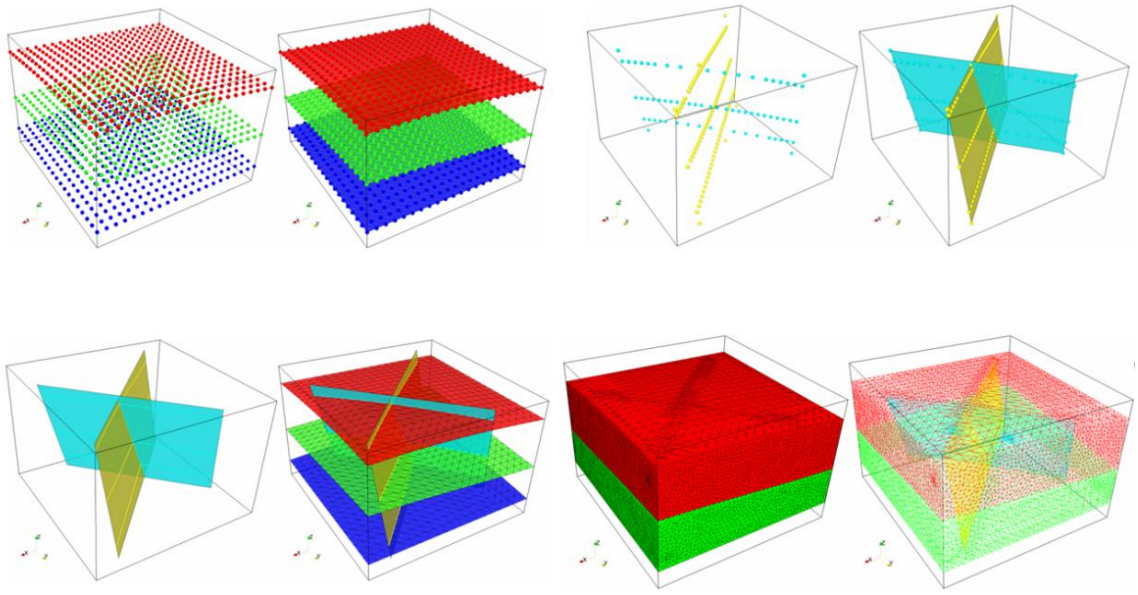

➔ *Figure 12: Exemplary mesh generation of a generic 3D FEM model with 2 units and 2 faults.*

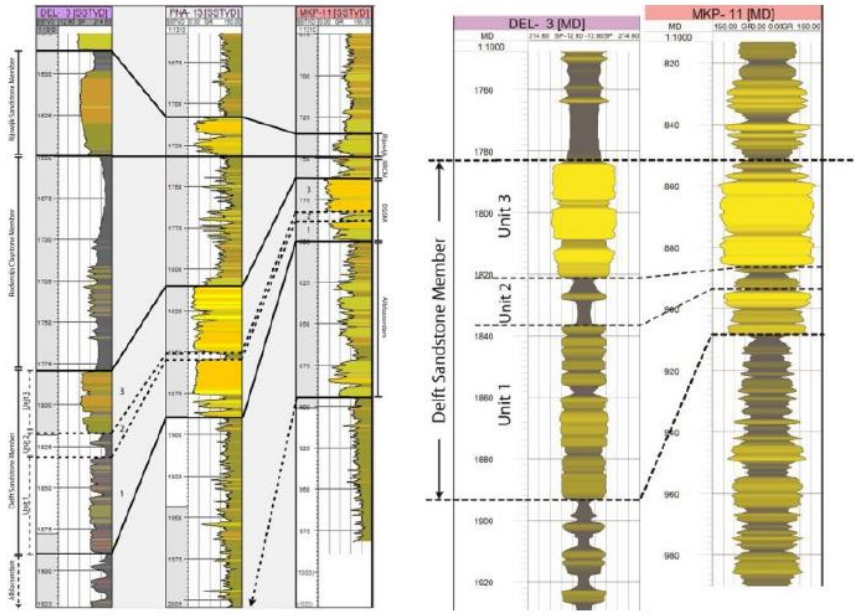

Figure 7: Left: Correlation panel through wells DEL-03, PNA-13 and MKP-11. Right: Subdivision of DSSM based on signature of SP-log (well DEL-03), gamma-ray log (well MKP-11), core and cuttings analyses. See Fig. 1 for well locations.

Figure 3 : (source: Donselaar et al (2015) - 12054.pdf)

Table 1
Performance indicators of WNB doublets. Grey italic values are derived from prognoses. R. GR: Rijnland Group aquifer, N. Fm. Nieuwerkerk Formation aquifer., Buntsst.: Buntsandstein aquifer.

Nr	Start	Aquifer	TVD [m]	Spacing (L) [km]	Area of influence (A) [km^2]	Production rate [m^3/h]	Production temperature [°C]	Screen length [m]	Capacity [MW]	MW/km^2
1	Aug-07	R. Gr.	1659	1.7	5.8	170	57	103	9	1.6
2	Sep-09	N. Fm.	1859.5	1.0	2.0	150	64	57	7.3	3.7
3	Aug-10	N. Fm.	2264	1.5	4.5	180	70	86	7	1.6
4	Dec-10	N. Fm.	2305	1.8	6.5	–	78	87	7	1.1
5	Feb-11	N. Fm.	2352.5	1.6	5.1	180	70	100	8	1.6
6	Jun-12	N. Fm.	2539	1.5	4.4	180	85	50	11.5	2.6
7	Sep-14	N. Fm.	2449	1.6	5.1	185	90	200	16	3.1
8	Oct-15	Buntsst.	2173	1.7	5.8	255	83	200	14	2.8
9	Dec-16	N. Fm.	2460	2.1	8.8	300	87	124	16	1.8
10	Mar-17	N. Fm.	2480	1.9	7.2	–	*85*	224	*16*	*2.2*
11	Nov-17	N. Fm.	–	–	–	–	*95*	–	*18*	–
12	Dec-17	N. Fm.	2473	1.5	4.5	360	87	83	21	4.7
13	Jan-18	N. Fm.	1855	1.6	5.4	360	65	93	15	2.8
Average			**2239**	**1.6**	**5.4**	**232**	**78**	**117**	**13**	**2.4**

Figure 4 : (source: Willems and Nick (2019) - 1-s2.0-S0306261919307469-main.pdf)

Note: only the N.Fm. (Nieuwerkerk Formation aquifer) is considered here

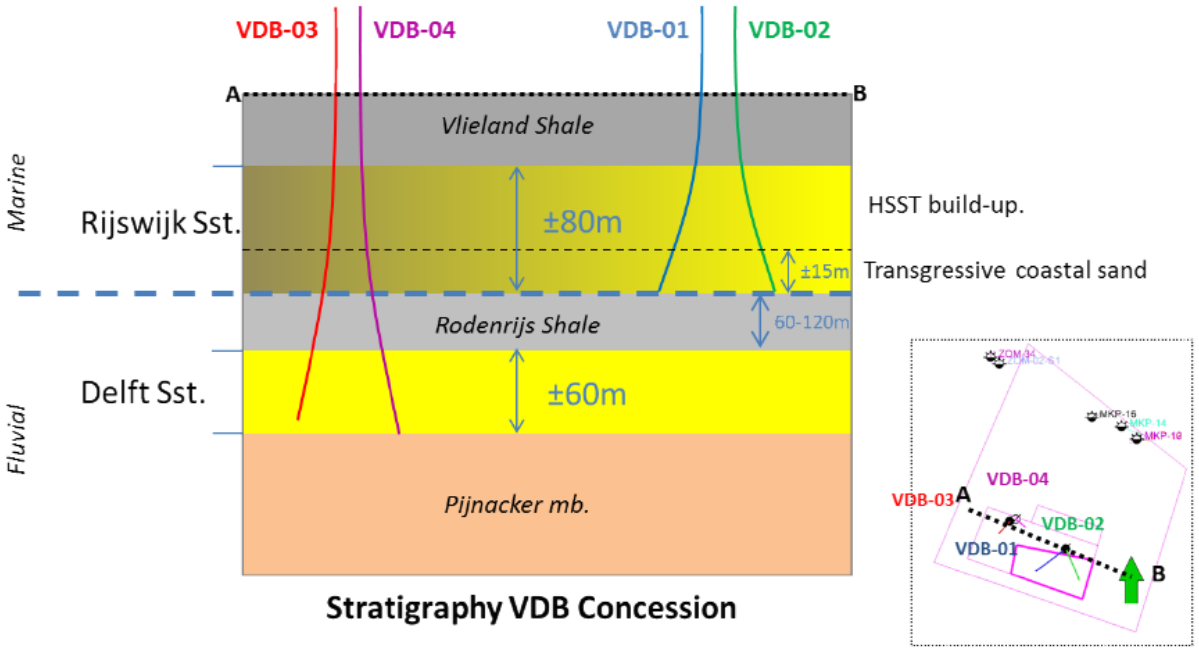

Figure 5-9 Schematic of the producing formations in the VDB concession.

Figure 5 : (source: Willems (2012) - Cees_Willems_thesis_lower_cretaceous_sands_WNB.pdf)

Note: only the N.Fm. (Nieuwerkerk Formation aquifer) is considered here

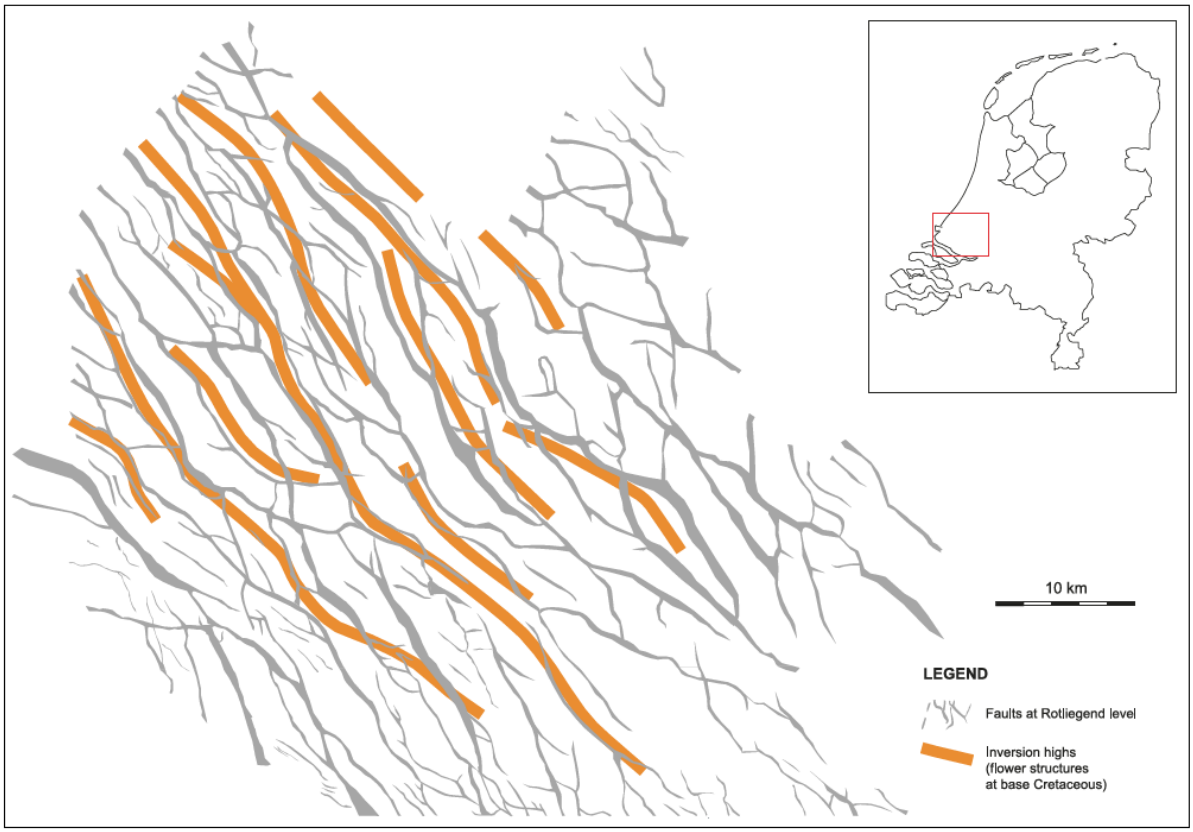

Figure 6 : (source: de Jager (2007) - 03GeologicalDevelopment-DeJager.pdf)

Note: only the N.Fm. (Nieuwerkerk Formation aquifer) is considered here

2. Rock mechanical data

For reservoir unit and adjacent formations (top and bottom layer)

Property (unit)	Mean value	Min. value	Max. value	Source
Young's modulus (GPa)				
Poisson's ratio (-)				
Tensile strength (MPa)				
UCS (MPa)				
Cohesion (MPa)				
Coefficient of internal friction (-)				
Coefficient of sliding friction (-)				
Matrix bulk modulus (GPa)				
Biot's coefficient (-)				

3. Hydraulic data

For reservoir unit and adjacent formations (top and bottom layer)

Property (unit)	Mean value	Min. value	Max. value	Source
Horiz. Permeability (mD)	1000	90 mD Careful: horiz. or vert. not specified	1130 mD Careful: horiz. or vert. not specified	"see text next to Figure 17" *Source: Donselaar et al (2015) - 12054.pdf* "see Figure 18" *Source: Willems and Nick (2019) - 1-s2.0-S0306261919307469-main.pdf*
Vert. Permeability (-)				
Porosity (-)	28%	19%	30%	"see text next to *Figure 17*" *Source: Donselaar et al (2015) - 12054.pdf* "see Figure 18" *Source: Willems and Nick (2019) - 1-s2.0-S0306261919307469-main.pdf*

3. GEOTHERMAL POTENTIAL

The geothermal potential of the DSSM depends on the total volume of potential reservoir sandstone, on the sandstone permeability and on the temperature of the formation water in the aquifer. Average net sand content (N/G) in the DSSM in the wells is about 0.65, and highest in Unit 3. A contour map of the top of the DSSM based on 3D seismic data shows that the depth of the DSSM is between 2000 m and 2300 m in the structural low beneath the license area (Fig. 8). Bottom-hole temperature readings from oil- and gas wells in the region indicate that the geothermal gradient is approximately 3°C/100m, which results in a temperature estimate of 65-75 °C for the formation water in the DSSM (Fig. 12). This is sufficient for use in a low-temperature grid-heating network or a glasshouse heating system. The permeability of the aquifer directly influences the production and re-injection flow rates. Appraisal drilling for hydrocarbons in and around the target area indicated that the DSSM has promising reservoir qualities, i.e., high porosity and permeability. Additional information on spatial and vertical variability was obtained from analyses on core samples and cuttings from wells MKP-11 in the Moerkapelle oil field (10 km to the northeast) and well DEL-03, which indicates that the three units identified in the DSSM have distinctly different porosity and permeability values. The average porosity of Unit 1 is about 19% and the permeability increases from about 90 mD at the base to 295 mD at the top of the unit. Unit 3 contains significantly coarser-grained material than Unit 1, and the average porosity is 30% and the permeability varies between 725 mD and 1130 mD, with the highest permeability found at the base. Unit 2 consists of very fine-grained sediment, has an extremely low porosity and permeability.

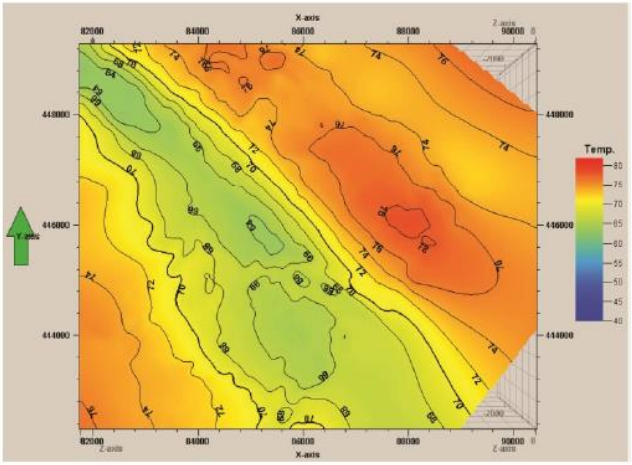

Figure 12: Temperature map of the top DSSM. Temperature in °C. Map constructed from interpreted seismic horizon top DSSM and applying the local thermal gradient of 3.11 °C per 100 m.

Figure 17 : (source: Donselaar et al (2015) - 12054.pdf)

Table 2
Aquifer and fluid properties used in the numerical simulations.

Property		Value	Units
Sandstone porosity	φ_{sst}	28	[%}
Shale porosity	φ_{sh}	10	[%}
Sandstone permeability	k_{sst}	1000	[mD]
Shale permeability	k_{sh}	1	[mD]
Specific heat capacity sandstone	C_{sst}	1.93	[MJ/m^3/K]
Specific heat capacity shale	C_{sh}	2.47	[MJ/m^3/K]
Thermal Conductivity Sandstone	λ_{sst}	2.7	[J/m/s/K]
Thermal Conductivity Shale	λ_{sh}	2	[J/m/s/K]
Density Sandstone	ρ_{sst}	2650	[kg/m^3]
Density Shale	ρ_{sh}	2600	[kg/m^3]

Figure 18 : (source: Willems and Nick (2019) - 1-s2.0-S0306261919307469-main.pdf)

Note: reservoirs correspond to sandstone intervals

4. Thermal data

For reservoir unit and adjacent formations (top and bottom unit). Temperature gradient may be the same in all units.

Property (unit)	Mean value	Min. value	Max. value	Source
Linear temperature gradient above top unit (°C/km) Linear temperature gradient in top unit (°C/km) Linear temperature gradient in reservoir unit (°C/km) Linear temperature gradient in bottom unit (°C/km)	3.11 °C/100m Careful: the unit is °C/100m 28.6°C/km			"see Fig.12 in Figure 17" *Source:* Donselaar et al (2015) - 12054.pdf "The calculated average geothermal gradients for the Rijnland and Schieland Groups are respectively 29.8 ℃/km and 28.6 ℃/km. This is relatively low in comparison to the 31,3 ℃/km geothermal gradient." *Source: Report_6425_Kennisagenda_V_2.1_def_FAULT.pdf (p.36)*
Thermal expansion coefficient (1/°C)				
Thermal conductivity (W/m/°C)	2.7 J/m/s/K Careful: ≠ unit			"see Figure 18" *Source: Willems and Nick (2019) - 1-s2.0-S0306261919307469-main.pdf*
Specific heat capacity (J/kg/°C)	1.93 MJ/m^3/K Careful: ≠ unit			"see Figure 18" *Source: Willems and Nick (2019) - 1-s2.0-S0306261919307469-main.pdf*
Matrix density (kg/m³)	2650 kg/m^3			"see Figure 18" *Source: Willems and Nick (2019) - 1-s2.0-S0306261919307469-main.pdf*
Heat flow (mW/m²)				

5. Fault property data

Property (unit)	Mean value	Min. value	Max. value	Source
Aperture at 0 MPa normal stress (m)				
Aperture at infinite normal stress (m)				
Dilation angle (°)				
Thickness (m)				
Porosity (-)				

Friction coefficient (-)				
Cohesion (MPa)				
Young's modulus (GPa)				
Poisson's ratio (-)				

6. Stress and pressure data

For reservoir unit, adjacent formations (top and bottom unit), and above (may be the same in all units)

Property (unit)	Mean value	Min. value	Max. value	Source
Max. Hor. Stress direction (° from N)	N135°E			Regarding the Northern German Basin: "Interestingly, the mean SH direction identified below the Zechstein salt layer seems to be roughly oriented in the N-S direction although it varies from N 30°E in the eastern part of the basin to the NW-SE direction (N135°E) in the westernmost part of the basin. This NW-SE direction is precisely the mean SH direction often accepted for North Western Europe (Mueller et al., 1992; Zang and Stephansson, 2010)." *Source: cornet-Roeckel-Stress profiles Europe.pdf (p.12)*
Pore pressure gradient above top unit (MPa/km)				See data regarding the West Netherlands Basin (WNB) in *Verweij et al.2016_vertical stress in the netherlands.pdf* "Above the salt, the pore pressure has been found to be close to hydrostatic equilibrium." -> statement for the Northern German Basin… *Source: cornet-Roeckel-Stress profiles Europe.pdf (p. 14)* "hydrostatic pressure gradient for any region is approximately 10.53 kPa/m" *Source: https://www.sciencedirect.com/topics/engineering/lithostatic-pressure*
Pore pressure gradient in top unit (MPa/km)				
Pore pressure gradient in reservoir unit (MPa/km)				
Pore pressure gradient in bottom unit (MPa/km)				
Min. hor. stress gradient above top unit (MPa/km)				

Min. hor. stress gradient in top unit (MPa/km)	0.1697 bar/m Careful: ≠ unit			"Based on our regional experience, we estimated a minimum horizontal stress gradient of 0.147 bar/m for the sandstone layers and 0.1697 for the shale layers." ->I think we can consider the above layer as a shale layer… *Source: stimulation_for_geothermal_wells_in_the_netherlands.pdf (p. 4)*
Min. hor. stress gradient in reservoir unit (MPa/km)	0.147 bar/m Careful: ≠ unit			"Based on our regional experience, we estimated a minimum horizontal stress gradient of 0.147 bar/m for the sandstone layers and 0.1697 for the shale layers." *Source: stimulation_for_geothermal_wells_in_the_netherlands.pdf (p. 4)*
Min. hor. stress gradient in bottom unit (MPa/km)	0.1697 bar/m Careful: ≠ unit			"Based on our regional experience, we estimated a minimum horizontal stress gradient of 0.147 bar/m for the sandstone layers and 0.1697 for the shale layers." ->I think we can consider the below layer as a shale layer… *Source: stimulation_for_geothermal_wells_in_the_netherlands.pdf (p. 4)*
Max. hor. stress gradient above top unit (MPa/km) Max. hor. stress gradient in top unit (MPa/km) Max. hor. stress gradient in reservoir unit (MPa/km) Max. hor. stress gradient in bottom unit (MPa/km)	16 MPa/km *--> which is < to the min horizontal stress gradient for shale layer mentioned above…..*			"We adopt parameters characteristic for Dutch reservoirs (…) a total vertical stress gradient of 0.023 MPa/m, a horizontal stress gradient of 0.016 MPa/m, and a hydrostatic pore pressure gradient of 0.011 MPa/m." *Source: 1-s2.0-S167477551630141X-main.pdf (p. 849 / 4)*
Vertical stress gradient above top unit (MPa/km) Vertical stress gradient in top unit (MPa/km) Vertical stress	< 23 MPa/km			See *Figure 19* "Fig. 22. Cross plot of lithostatic pressure versus depth at Q13-04 in the inverted WestNetherlands Basin (WNB) showing that at

gradient in reservoir unit (MPa/km)				depths of less than 2.5 km the lithostaticgradient is slightly lower than the standard gradient and that it follows the standardgradient at greater depths." ➔ The often used standardvertical stress gradient (also referred to as lithostatic pressuregradient) of 23 MPa/km (~1 psi/ft) corresponds to an average bulk density of about 2300 kg/m3 for clastic rocks with a water-filled porosity of 15%. (page 871 / 2) *Source: Verweij et al.2016_vertical stress in the netherlands.pdf*
Vertical stress gradient in bottom unit (MPa/km)				

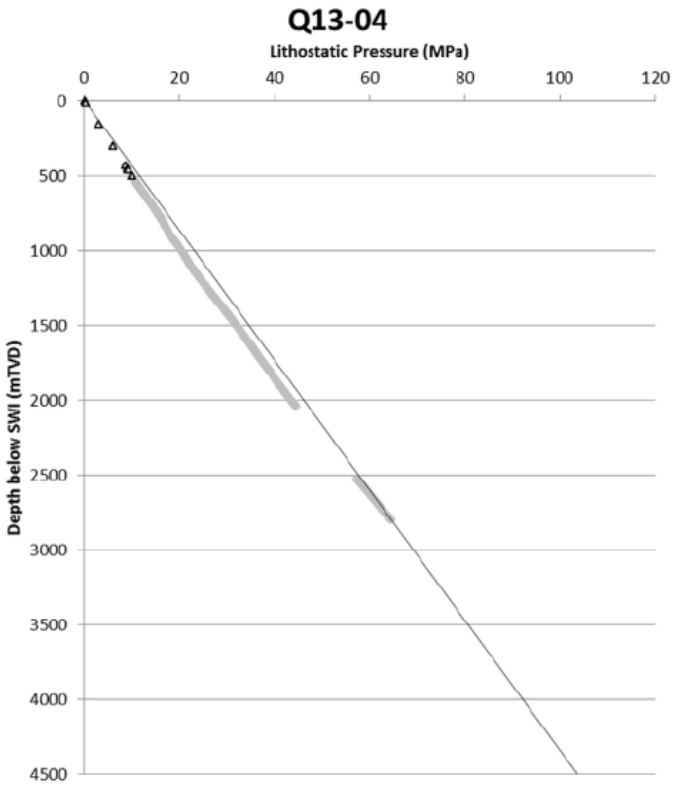

Fig. 22. Cross plot of lithostatic pressure versus depth at Q13-04 in the inverted West Netherlands Basin (WNB) showing that at depths of less than 2.5 km the lithostatic gradient is slightly lower than the standard gradient and that it follows the standard gradient at greater depths. The Cenozoic North Sea Supergroup is relatively thin and the Chalk Group is missing by erosion in the inverted part of the basin and the non-salt fringe Zechstein Group sediments are less than 20 m thick.

Figure 19 : source: Verweij et al.2016_vertical stress in the netherlands.pdf

7. Reservoir fluid data

Reference temperature: 20°C

Property (unit)	Mean value	Min. value	Max. value	Source
Density (kg/m³)	1.091 g/cm^3 Careful: ≠ unit			"See *Figure 20*." *source: Puttest1-GWW-BWG Geochemische beratung report.pdf*
Viscosity (mPas)				
Thermal expansion coefficient (1/°C)				
Specific heat capacity (J/kg/°C)				
Thermal conductivity (W/m/°C)				

Salinity (g/L)				
Bulk modulus (GPa)				

Table 1: Physico-chemical properties

Denomination		HON GT1-070312	HON GT1-080312	HON GT1-080312
Date of sampling	unit	07.03.2012 6:40 p.m.	08.03.2012 1:30 p.m.	08.03.2012 4:30 p.m.
Temperature	°C		85.8	86.1
Production rate	l/s		43.3	43.4
Production amount	m³		3,940	4,250
Parameter				
Colour		yellowish (very low oil layer)		
Turbidity		none		
Smell		specific, little by hydrocarbons		
Precipitate		in air brown solids		
Degassing		yes		
Sample temperature	°C	81.3	81.4	83.7
pH value at sample temperature		6.18	6.01	6.01
pH value at 20.0°C		6.20	n.b.	5.96
Redox potential measured for Ag/AgCl	mV	-268	-265	-282
Redox potential SHE	mV	-93	-90	-109
Oxygen (O_2)	mg/l	<1	<1	<1
Conductivity on site	mS/cm	145.0	n.b.	141.7
Conductivity (25°C) at laboratory	mS/cm	165.4	n.b.	166.5
Density 20°C	g/cm³	n.b.	n.b.	1.091
Acid capacity pH 4,3	mmol/L	2.68	n.b.	2.48
Base capacity pH 8,2	mmol/L	5.35	n.b.	5.15
Sulphide	mg/L	undetectable		

Figure 20 : source: Puttest1-GWW-BWG Geochemische beratung report.pdf

Honselersdijk geothermal production field

Reference temperature: mean reservoir temperature

70°C for the Van den Bosch Geothermal energy concession *source: Willems (2012) - Cees_Willems_thesis_lower_cretaceous_sands_WNB.pdf – page 91 (VDB-03 bottom hole temp.).*

Property (unit)	Mean value	Min. value	Max. value	Source
Density (kg/m³)	1.034 sg Careful: ≠ unit			"See *Figure 21*." *Source: stimulation_for_geothermal_*

				wells_in_the_netherlands.pdf
Viscosity (mPas)	0.367 cp Careful: ≠ unit			"See *Figure 21*." *Source: stimulation_for_geothermal_wells_in_the_netherlands.pdf*
Thermal expansion coefficient (1/°C)				
Specific heat capacity (J/kg/°C)				
Thermal conductivity (W/m/°C)				
Salinity (g/L)				
Bulk modulus (GPa)				

Table 3. Fluid properties for den Haag analogue

Parameter	Producer well	Injector well
Reservoir pressure (bar)	219	179
Water viscosity (cp)	0.367	0.626
Water density (sg)	1.034	1.069
Temperature (°C)	73	40

Figure 21 : (source: de Pater and Shaoul (2020) - stimulation_for_geothermal_wells_in_the_netherlands.pdf)

8. Seismological data

Property (unit)	Mean value	Min. value	Max. value	Source
Criticality C(z) (Pa)				
Seismogenic index Σ (-)				
b-value (-)				

9. Operation/wellbore data

Property (unit)	Mean value	Min. value	Max. value	Source
Distance between injector and producer (m)	1600	1000	2100	"see Figure 4" + description in the text *Source: Willems and Nick (2019) - 1-s2.0-S0306261919307469-main.pdf*
Injection temperature (°C)	35°C			*Source: Willems and Nick (2019) - 1-s2.0-S0306261919307469-main.pdf (p. 586)*

	30°C			VDB-04 Injection well *source: Willems (2012) - Cees_Willems_thesis_lower _cretaceous_sands_WNB.pdf page 91*
Flow rate (l/s)	237 m^3/h Careful: the unit is m^3/h	150 m^3/h Careful: the unit is m^3/h	360 m^3/h Careful: the unit is m^3/h	"see Figure 4" + description in the text *Source: Willems and Nick (2019) - 1-s2.0-S0306261919307469-main.pdf*
Length of perforated/open interval (m)				See documents in the "Green Well Westland" folder. Data from the Honselersdijk geothermal production field. See from page 94 for well information *source: Willems (2012) - Cees_Willems_thesis_lower _cretaceous_sands_WNB.pdf*
Inner diameter wellbore (m)				See documents in the "Green Well Westland" folder. Data from the Honselersdijk geothermal production field. See from page 94 for well information *source: Willems (2012) - Cees_Willems_thesis_lower _cretaceous_sands_WNB.pdf*

Appendix B

Slochteren Formation

t

GFZ
Helmholtz Centre
POTSDAM

HELMHOLTZ CENTRE POTSDAM
GFZ GERMAN RESEARCH CENTRE
FOR GEOSCIENCES

Dr. Hannes Hofmann

Section 4.8

Telegrafenberg

hannes.hofmann@gfz-potsdam.de

Telephone: +49 (0)331 288-28739

Potsdam, 07 September 2020

Data requirements for KEM-15 ("Cooling induced seismicity")

This document contains a list of data reqired to perform the numerical simulations of cooling induced seismicity using the Finite Element Code GOLEM. The model is based on the published and history matched GOLEM model of Groß Schönebeck Enhanced Geothermal System. Based on this model up to 5 generic and specific models will be built:

1 generic hydrothermal model (shallower, no stimulated fractures)
1 generic EGS model (deeper, with stimulated fractures)
1 specific hydrothermal reservoir above salt in the Netherlands
1 specific hydrothermal reservoir below salt in the Netherlands
1 specific deep EGS reservoir in the Netherlands

This document concerns the hydrothermal reservoir below the Permian salt in the Netherlands. The considered reservoir formation is the **Slochteren Formation** which is part of the Upper Rotliegend Group.
The Zechstein Group is used as the top layer (parameter values may refer to anhydrite, halite or unspecified rocks).
The Carboniferous (Limburg Group) is used as the bottom layer.

The Slochteren sandstone of the Upper Rotliegend Group forms to the Groningen reservoir. Many of the parameter values added into the following tables mostly refer to data provided by the Groningen gas field. Geothermal production field exploiting Rotliegend reservoir are also located in the northern part of the Netherlands.

Parameter values indicated in this document correspond to "geological" information (from well / care / sample analysis). Values derived from or used in modelling studies are not indicated in here.

For each of these models the parameter list below is required.

10.Geological models (geometry)

For the specific reservoir models a GOCAD (*.gp) file of the reservoir geometry would be best. Alternatively, the individual faults, surfaces and well paths may be provided as point data (X, Y, Z). For the generic models the table below is enough.

Property (unit)	Mean value	Min. value	Max. value	Source

Reservoir unit top (m)	2200	1500	3000	Middenmeer. *http://www.destress-h2020.eu/en/demonstration-sites/middenmeer/* *https://wellengineeringpartners.com/geothermal-ecw-middenmeer-two-doublets-delivery/* "Eight geothermal systems have Slochteren Sandstone as reservoir (MEA, 2018). Target depths are between 1.5 and 3 km. « *Introduction_to_the_geothermal_play_and_reservoir_.pdf* (p.14)
Reservoir unit thickness (m)	200	100	250	Middenmeer. *http://www.destress-h2020.eu/en/demonstration-sites/middenmeer/* *Introduction_to_the_geothermal_play_and_reservoir_.pdf* (p.15) --> Slochteren Formation of the Upper Rotliegend Group for the 8 geothermal systems in the NL.
Top layer thickness (m)	200			Corresponds to the Zechstein Group *https://www.dinoloket.nl/en/subsurface-models*
Bottom layer thickness (m)	600			Corresponds to the Carboniferous (Limburg Group) *https://www.dinoloket.nl/en/subsurface-models*
# of fault sets	2			"see *Figure 6*" *Source: de Jager (2007) - 03GeologicalDevelopment-DeJager.pdf* N130°E been the dominant base on a national scale map --> scale / resolution issue *DUIN et al_2006_ID21237.pdf*
Fault set strike (° from N)	N130°E & N150°E			
Fault set dip (° from hor.)	80°			▪ Strike-slip faults are usually subvertical faults, if we consider these faults been strike-slip…
Fault set dip direction (° from N)	N040°E - N220°E & N060°E - N240°E			"see *Figure 6*" *Source: de Jager (2007) - 03GeologicalDevelopment-DeJager.pdf*
Fault length (m)	25 000	10 000	>60 000	"see *Figure 6*" *Source: de Jager (2007) - 03GeologicalDevelopment-DeJager.pdf*
Fault spacing (m)	5000m for the main faults			"see *Figure 6*"

				Source: de Jager (2007) - 03GeologicalDevelopment-DeJager.pdf
Units intersected by fault				Presumably all 3 layers considered in the model (bottom, reservoir and top layers)

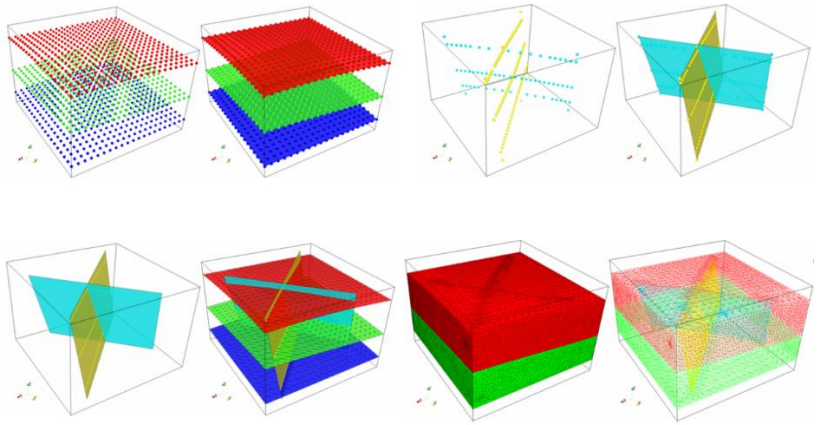

- *Figure 22: Exemplary mesh generation of a generic 3D FEM model with 2 units and 2 faults.*

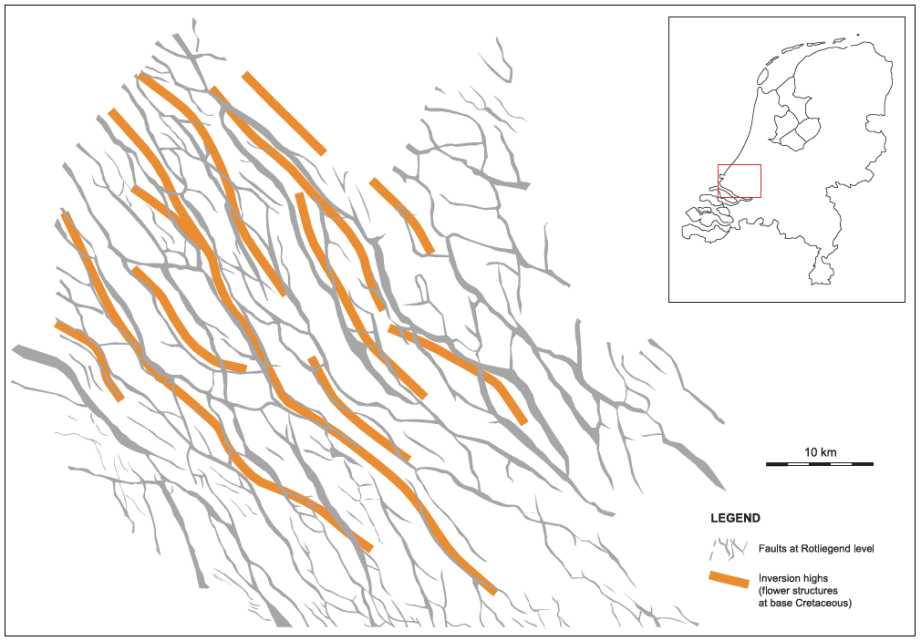

Figure 23 : (source: de Jager (2007) - 03GeologicalDevelopment-DeJager.pdf)

Note: this map is not coming from an area where Slochteren reservoir is used for geothermal energy. Main fault trend can however be applied further north

11.Rock mechanical data

For reservoir unit and adjacent formations (top and bottom layer)
For Permian reservoir - Slochteren Formation part of the Upper Rotliegend Group

Property (unit)	Mean value	Min. value	Max. value	Source
Young's modulus (GPa)	13.5	2.6	34.8	Values interpreted from *Figure 24* See *Table 1* line 1 for more details
Poisson's ratio (-)	0.18	0.02	0.28	Values interpreted from *Figure 24*. Mean value emphasised by Figure 28 See *Table 1* line 2 for more details
Tensile strength (MPa)				
UCS (MPa)	?	5	39	See *Table 1* line 3 for more details
Cohesion (MPa)	4.5	1.25	8.1	Values from Figure 29 See *Table 1* line 4 for more details
Coefficient of internal friction (-)	0.53	0.45	0.63	Values from Figure 28 See*Table 1* line 6 for more details
Coefficient of sliding friction (-)				
Matrix bulk modulus (GPa)				
Biot's coefficient (-)	0.8	0.52	0.97	Values interpreted from *Figure 24* See *Table 1* line 7 for more details

- *Table 1: Rock mecanical data additional information*

Properties (unit)	Value	Description	
Young's modulus (Pa)	See estimated values from EKL-12 and ZPD-12 wells (Figure 15)	"Across the reservoir formation, the Young's modulus has been estimated using the relationship derived from laboratory tests of young's modulus and porosity carried out in the wells Eemskanaal-12 and Zuiderpolder-12." *Source: NAM (2015) Groningen 2015 Geomechanical Analysis*	1
	Porosity-Dependent	Values for stratigraphic intervals above and below the reservoir are presented in *Figure 24* below *Source: NAM (2015) Groningen 2015 Geomechanical Analysis*	
Poisson ratio (-)	See values derived from data from 13 wells across Groningen field (Figure 28)	Figure 28 - Details for the equations used to calculate the Poisson ratio are presented in section 2.3.2. of *NAM (2015) Dynamic Geomechanical Modelling to Assess and Minimize the Risk for Fault Slip during Reservoir Depletion of the Groningen Field*	2
	Porosity-Dependent	Values for stratigraphic intervals above and below the reservoir are presented in *Figure 24* *Source: NAM (2015) Groningen 2015 Geomechanical Analysis*	
Uniaxial compressive strength (Pa) Uniaxial Compressive Strength also known as the Unconfined Compressive Strength (UCS) Careful: Values are from very deep samples (~ 2 700 to 3 700 m)	9 – 10 MPa	"the average rock strength across the sand was estimated to be around 9 – 10 MPa." See values from the Uiterburen-10 well in Figure 16. *Source: NAM (2015) Dynamic Geomechanical Modelling to Assess and Minimize the Risk for Fault Slip during Reservoir Depletion of the Groningen Field*	3
	15 – 26 MPa	"the average rock strength for the Slochteren formation is around 15 – 26 MPa in the Loppersum area." Values from ZND-12 well. *Source: NAM (2015) Dynamic Geomechanical Modelling to Assess and Minimize the Risk for Fault Slip during Reservoir Depletion of the Groningen Field*	
	See other values from acoustic logs data from 13 wells across Groningen field (Figure 17)	*Source: NAM (2015) Dynamic Geomechanical Modelling to Assess and Minimize the Risk for Fault Slip during Reservoir Depletion of the Groningen Field*	
	See values from additional 3 wells (FRB-8, ZND-12 and ZDV-6) in Figure 29	*Source: NAM (2015) Dynamic Geomechanical Modelling to Assess and Minimize the Risk for Fault Slip during Reservoir Depletion of the Groningen Field*	

Cohesion (Pa)	See values from 3 wells (FRB-8, ZND-12 and ZDV-6) in Figure 29	*Source: NAM (2015) Dynamic Geomechanical Modelling to Assess and Minimize the Risk for Fault Slip during Reservoir Depletion of the Groningen Field*	*4*
Internal friction angle (Deg.) ➔ Parameter not listed initially	See values from 3 wells (FRB-8, ZND-12 and ZDV-6) in Figure 29	*Source: NAM (2015) Dynamic Geomechanical Modelling to Assess and Minimize the Risk for Fault Slip during Reservoir Depletion of the Groningen Field*	*5*
Friction coefficient (-)	See values derived from data from 13 wells across Groningen field (Figure 28)	Figure 28 - Details for the equations used to calculate the Poisson ratio are presented in section 2.3.2. of *NAM (2015) Dynamic Geomechanical Modelling to Assess and Minimize the Risk for Fault Slip during Reservoir Depletion of the Groningen Field*	6
Biot coefficient	Ranged from 0.7 to 0.9 See graph Figure 20	"The Biot coefficient is generally stress insensitive and ranged from 0.7 – 0.9 for most samples. A few high porosity samples displayed decreasing Biot coefficients with stress and were also much lower, with value range 0.4 – 0.7." *Source: NAM (2019) Groningen Geomechanical Laboratory Testing of the Zeerijp-3A Compaction study*	7
	Porosity-Dependent	Values for stratigraphic intervals above and below the reservoir are presented in *Figure 24* *Source: NAM (2015) Groningen 2015 Geomechanical Analysis*	

Unit		Young's Modulus (GPa)	Poisson's Ratio	Density (kg/m^3)	Data Source
North Sea		2	0.3	2150	NAM
Chalk		10	0.25	2350	NAM
Rijnland		16	0.25	2350	NAM
Triassic		16	0.25	2350	NAM
Zechstein	Halite	30	0.35	2100	NAM
	Andydrite	70	0.25	2900	Literature
Ten Boer		40	0.2	2300	NAM
Slochteren	Heterolithic	Porosity-Dependent			Same properties as reservoir used
	Reservoir				Core Data
Carboniferous		40	0.2	2300	NAM

Table 1.1. Elastic material properties and densities for rock layers.

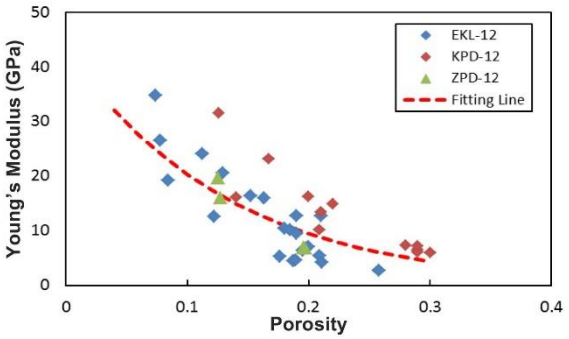

Fig. 1.2. Young's modulus vs. porosity of the reservoir rock.

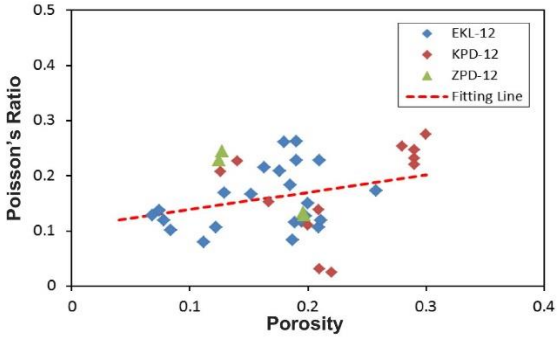

Fig. 1.3. Poisson's ratio vs. porosity of the reservoir rock.

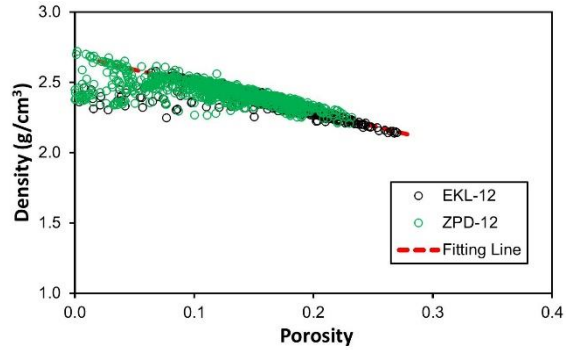

Fig. 1.4. Density vs. porosity of the reservoir rock.

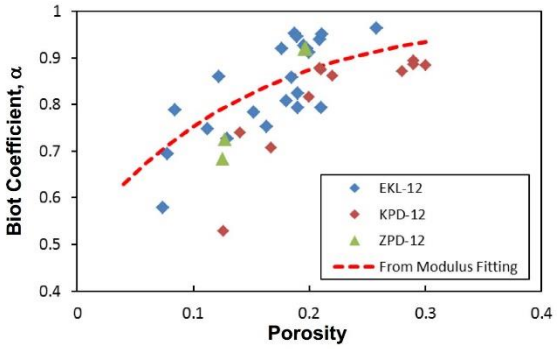

Fig 1.5. Biot coefficient vs. porosity for the reservoir rock.

Figure 24 : (source: NAM (2015) Groningen 2015 Geomechanical Analysis)

Table 10. EKL-12 and ZPD-12 laboratory Young's Modulus and Porosity (courtesy of NAM[7])

Well	TVD (m)	E (Mpa)	Porosity (%)
EKL-12	2740	14704	0.4
	2744.7	12728	6.8
	2751.8	4441	18.7
	2760	6388	19.5
	2761.5	4652	18.9
	2770.4	2660	25.8
	2798.9	5457	20.9
	2800.3	4238	21.1
	2812.8	16039	16.3
	2813.7	6785	19.8
	2715.3	10472	18
	2815.9	10202	18.5
	2815.9	9529	19
	2835.4	26581	7.8
	2840.6	16378	15.2
	2850.4	20616	12.9
	2859	12635	12.2
	2868.4	19253	8.4
	2872.6	25823	7.4
	2876.6	34813	7.4
	2900.9	24171	11.2
ZPD-12	2756	6856	19.6
	2756	6737	19.7
	2837.4	19642	12.1
	2837.4	15977	12.7

Figure 15 : (source: NAM (2015) Dynamic Geomechanical Modelling to Assess and Minimize the Risk for Fault Slip during Reservoir Depletion of the Groningen Field)

Table 7. Uiterburen-10 Uniaxial strength data (provided by NAM through electronic communication, e-mail).

UTB-10	
Original Core Depth (AHDD)	UCS
m	*bar*
3131.80	71
3132.86	25
3140.47	92
3142.25	33
3142.99	65
3143.24	104
3143.56	94
3143.56	55
3146.25	116
3149.20	129
3159.11	49
3159.37	37
3159.37	92
3163.21	30
3163.53	36
3172.14	68
3173.29	177
3176.82	56
3181.08	17
3181.36	154
3182.49	87
3193.17	64
3193.94	36
3194.37	25
3194.62	24
3198.60	291
3200.04	11
3201.54	42
3206.94	81
3234.52	392
3239.97	242

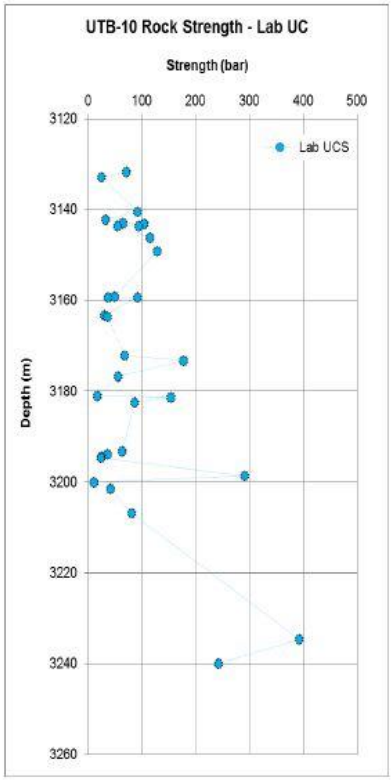

Figure 16 : (source: NAM (2015) Dynamic Geomechanical Modelling to Assess and Minimize the Risk for Fault Slip during Reservoir Depletion of the Groningen Field)

Table 8. UCS statistic summary for ROSLN and Carboniferous

Well	UCS ROSLN - Sand				UCS Carboniferous - Shale			
	Pmin	P10	P50	P90	Pmin	P10	P50	P90
BRW-2	15.89	20.68	25.12	29.13	11.16	12.78	19.87	23.53
EKL-1	8.89	14.58	19.57	28.45	No coverage			
HGZ-1	13.35	17.62	23.04	27.47	11.18	18.42	23.82	27.91
KWR-1A	18.89	24.64	31.1	37.57	3.94	14.28	20.85	25.28
OVS-1	8.9	14.78	19.25	30.06	12.7	14.96	15.97	18.45
POS-1	9.47	12.5	16.63	30.82	14.33	14.85	16.5	17.17
RDW-1	11.2	17.11	22.17	29.16	13.99	16.35	18.85	21.8
SLO-3	9.13	11.24	17.08	30.33	6.44	12.24	16.43	18.99
UHM-1A	12.02	17.84	23.6	31.69	No coverage			
ZND-1	2.63	14.23	18.85	30.26	No coverage			
ZPD-1	10.46	19.16	24.28	29.47	4.89	10.76	18.07	21.91
ZRP-1	12.65	16.86	24.89	32.65	16.69	17.97	19.86	21.28
ZWD-1	18.94	24.47	30.42	38.05	9.7	14.13	21.63	25.62

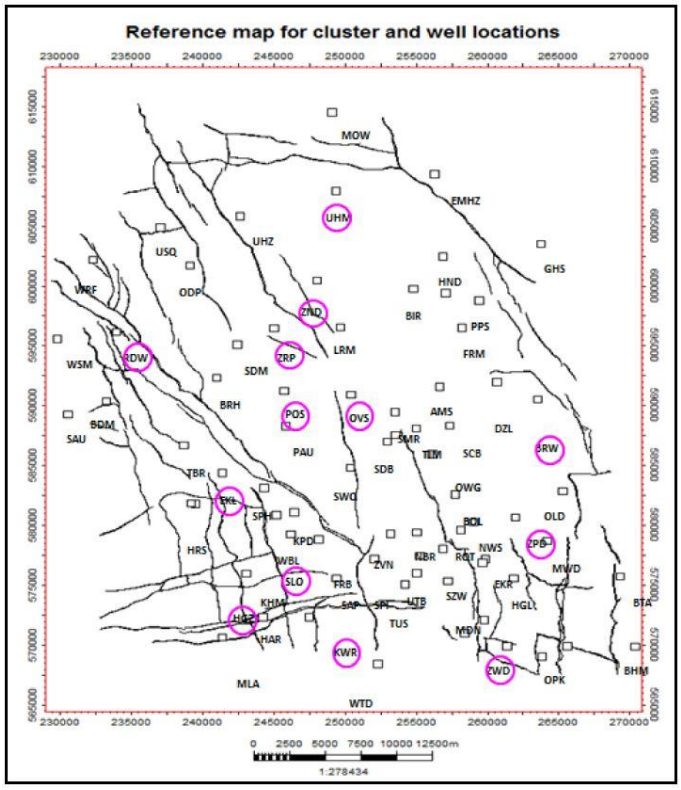

Wells location map

Borgsweer (BRW-2), Eemskanaal (EKL-1)
Hoogezand (HGZ-1), Kielwindeweer (KWR-1A)
Overschild (OVS-1), Ten Post (POS-1)
Rodewolt (RDW-1), Slochteren (SLO-3)
Uithuizermeeden (UHM-1A), T Zand (ZND-1)
Zuiderpolder (ZPD-1), Zeerijp (ZRP-1)
Zuidwending (ZWD-1)

Figure 17 : (source: NAM (2015) Dynamic Geomechanical Modelling to Assess and Minimize the Risk for Fault Slip during Reservoir Depletion of the Groningen Field)

ROSLN = Rotliegend Group / Slochteren Formation

The results of Pmin, P10, P50 and P90 indicate respectively the minimum, 10%, 50% and 90% of the rock strength, commonly presented in probabilistic analysis.

Table 9. Internal Friction and Poisson Ratio values for Halite, ROCLT, ROSLN and DC using equation 9, 10 and 11.

Well	Internal Friction			Poisson Ratio			
	Halite	ROSLN	ROCLT/DC	Halite	ROCLT	ROSLN	DC
BRW-2	0.82	0.56	0.56	0.25	0.26	0.18	0.23
EKL-1	0.82	0.5	0.5	0.25	0.27	0.18	N/A
HGZ-1	0.82	0.45	0.5	0.25	0.22	0.18	0.21
KWR-1A	0.82	0.45	0.5	0.25	0.21	0.18	0.23
OVS-1	0.82	0.63	0.56	0.25	0.28	0.18	0.26
POS-1	0.82	0.53	0.56	0.25	0.27	0.18	0.26
RDW-1	0.82	0.53	0.56	0.25	0.24	0.18	0.23
SLO-3	0.82	0.53	0.5	0.25	0.29	0.18	0.26
UHM-1A	0.82	0.53	0.55	0.25	0.25	0.18	N/A
ZND-1	0.82	0.6	0.5	0.25	0.27	0.18	N/A
ZPD-1	0.82	0.53	0.55	0.25	0.27	0.18	0.25
ZRP-1	0.82	0.55	0.55	0.25	0.26	0.18	0.26
ZWD-1	0.82	0.53	0.6	0.25	0.24	0.18	0.23

Figure 28 : (source: NAM (2015) Dynamic Geomechanical Modelling to Assess and Minimize the Risk for Fault Slip during Reservoir Depletion of the Groningen Field)

ROSLN = Rotliegend Group / Slochteren Formation; ROCLT = Rotliegend Group / Ten Boer Member; DC = Carboniferous.
See wells location map in Figure C.

Table 6. Summary of interpreted triaxial tests for FRB-8, ZND-12 and ZLV-6

Well	Depth MD (m)	UCS (Mpa)	Internal Friction (deg)	Cohesion (MPa)	Comments	Tested depth
FRB-8	2756.84 - 2757.35	21.4	19.33	7.59	Interval 1	Reservoir
	2760.95 - 2761.16	5.44	31.38	1.53	Interval 2	Reservoir
	2756.81 - 2761.16	16.95	23.73	5.53	Complete Interval	Reservoir
ZND-12	2816.47 - 2818.85	5.96	44.42	1.25	Interval 1	Reservoir
	2819.10 - 2820.33	24.36	22.73	8.1	Interval 2	Reservoir
	2816.47 - 2820.33	14.84	29.39	4.34	Complete Interval	Reservoir
ZDV-6	3795.96 - 3796.26	14.94	35.24	3.87	Interval 1	Reservoir
	3796.38 - 3797.22	14.41	30.61	4.11	Interval 2	Reservoir
	3795.96 - 3797.22	15.3	32.05	4.24	Complete Interval	Reservoir

Figure 29 : (source: NAM (2015) Dynamic Geomechanical Modelling to Assess and Minimize the Risk for Fault Slip during Reservoir Depletion of the Groningen Field)

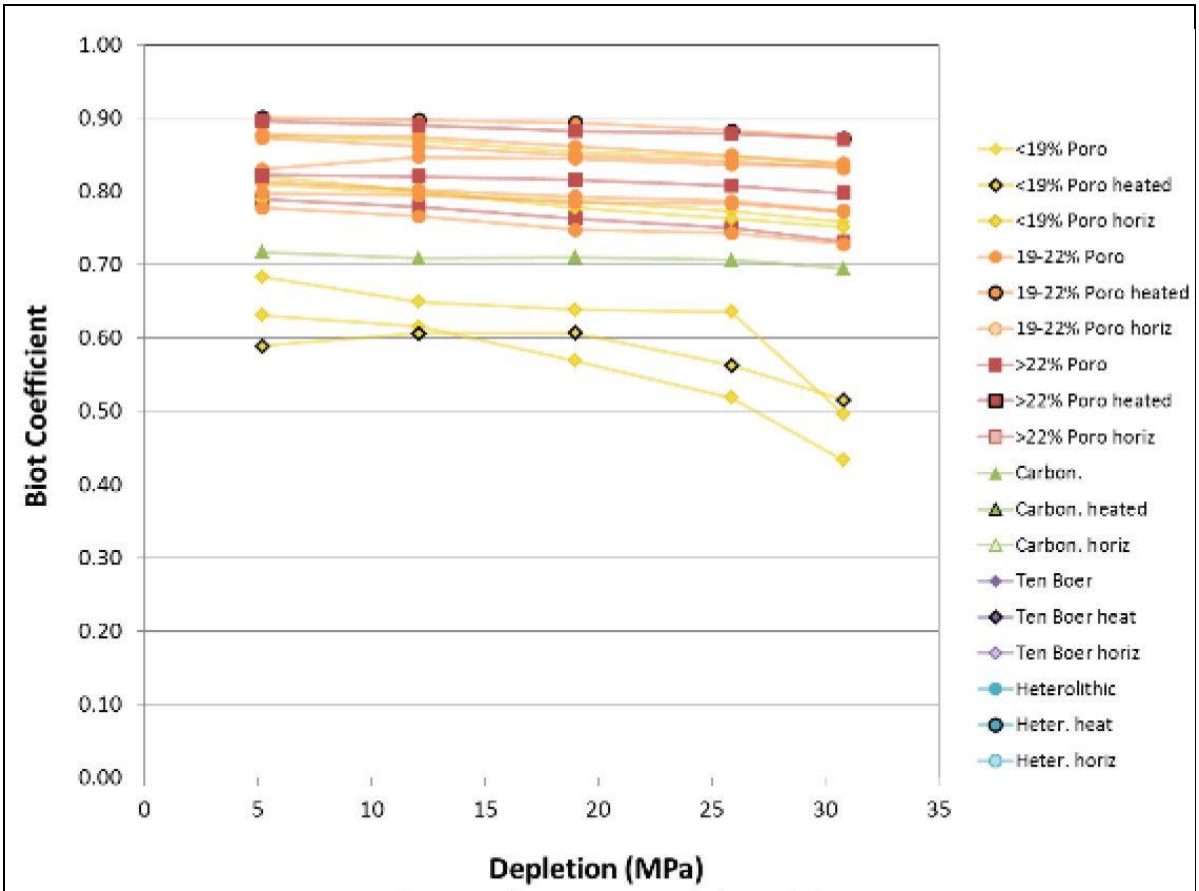

Figure 5. Biot coefficient measurend during UXS testing.

Figure 20 : (source: NAM (2019) Groningen Geomechanical Laboratory Testing of the Zeerijp-3A Compaction study)

For top layer: Zechstein Group

Property (unit)	Mean value	Min. value	Max. value	Source
Young's modulus (GPa)	70 (anhydrite) 30 (halite)			see *Figure 24*
Poisson's ratio (-)	0.25 (anhydrite) 0.35 (halite)			see *Figure 24*
Tensile strength (MPa)				
UCS (MPa)				
Cohesion (MPa)				
Coefficient of internal friction (-)	0.82 (halite)			Values from Figure 28
Coefficient of sliding friction (-)				
Matrix bulk modulus (GPa)				
Biot's coefficient (-)				

For bottom layer: Carboniferous (Limburg Group)

Property (unit)	Mean value	Min. value	Max. value	Source
Young's modulus (GPa)	40			see Figure 24

Poisson's ratio (-)	0.24 0.2	0.21	0.26	Values from Figure 28 Figure 24.
Tensile strength (MPa)				
UCS (MPa)	See values from acoustic logs data from 13 wells (Figure 17)			*Source: NAM (2015) Dynamic Geomechanical Modelling to Assess and Minimize the Risk for Fault Slip during Reservoir Depletion of the Groningen Field*
Cohesion (MPa)				
Coefficient of internal friction (-)	0.54	0.5	0.6	Values from Figure 28
Coefficient of sliding friction (-)				
Matrix bulk modulus (GPa)				
Biot's coefficient (-)				

12.Hydraulic data

For reservoir unit and adjacent formations (top and bottom layer)

Property (unit)	Mean value	Min. value	Max. value	Source
Horiz. Permeability (mD)		50	350	*Introduction_to_the_geothermal_play_and_reservoir_.pdf* (p.15) --> Slochteren Formation of the Upper Rotliegend Group for the 8 geothermal systems in the NL.
	100 mD			*2016.01.04_bia debietverhoging 2-4km_report.pdf* (p.35) --> Middenmeer concession, Slochteren Formation of the Upper Rotliegend Group.
	240			*spba-chapter7.pdf* (p.19) --> Permeability and porosity values are indicated for the Slochteren Fm. of the Groningen gaz field (table 7.5)
	Variable			"see *Figure 17*" *Source: 1-s2.0-S0375650516300700-main.pdf (p.2)*
	297 mD			*Source: Doddema (2012); 148285679.pdf (p.23)*
	250 mD			"see *Figure 22*" *Source: Doddema (2012); 148285679.pdf*
Vert. Permeability (-)	250 mD			"see *Figure 22*" *Source: Doddema (2012); 148285679.pdf* "The lack of data for vertical permeability was accounted for in the model by consistently assigning a vertical permeability which was one order of magnitude lower than the respective horizontal permeability (Carlson, 2003).This is a worst case estimate compared to the Kx/Kz ratio of 1.7usually used for the Rotliegend (van Leeuwen et al., 2014)" *Source: 1-s2.0-S0375650516300700-main.pdf (p.7)*

Porosity (-)	16 – 17 %	10 %	20%	*Thesis_Report_Redjosentono.pdf* (p.63) --> Koekoekspolder Geothermal project; Rotliegend eolian sandstone, Slochteren Formation of the Upper Rotliegend Group *spba-chapter7.pdf* (p.19) --> Permeability and porosity values are indicated for the Slochteren Fm. of the Groningen gaz field (table 7.5)

For top layer: Zechstein Group

Property (unit)	Mean value	Min. value	Max. value	Source
Horiz. Permeability (mD)	10^{-10} 0			"see *Figure 17*" *Source: 1-s2.0-S0375650516300700-main.pdf* "see *Figure 22*" *Source: Doddema (2012); 148285679.pdf (p.23)*
Vert. Permeability (-)	0			"see *Figure 22*" *Source: Doddema (2012); 148285679.pdf*
Porosity (-)	1% 0%			"see *Figure 17*" *Source: 1-s2.0-S0375650516300700-main.pdf* "see *Figure 22*" *Source: Doddema (2012); 148285679.pdf*

For bottom layer: Carboniferous (Limburg Group)

Property (unit)	Mean value	Min. value	Max. value	Source
Horiz. Permeability (mD)	10^{-2} 0			"see *Figure 17*" *Source: 1-s2.0-S0375650516300700-main.pdf* "see *Figure 22*" *Source: Doddema (2012); 148285679.pdf*
Vert. Permeability (-)	0			"see *Figure 22*" *Source: Doddema (2012); 148285679.pdf*
Porosity (-)	1% 0%			"see *Figure 17*" *Source: 1-s2.0-S0375650516300700-main.pdf* "see *Figure 22*"

				Source: Doddema (2012); 148285679.pdf

13.Thermal data

For reservoir unit and adjacent formations (top and bottom unit). Temperature gradient may be the same in all units.

Property (unit)	Mean value	Min. value	Max. value	Source
Linear temperature gradient above top unit (°C/km)	31 °C/km			"The average geothermal gradient in the Netherlands in 31°C/km with an average surface temperature of 10°C (Bonté et al, 2012). " *Introduction_to_the_geothermal_play_and_reservoir_.pdf (p.7)*
Linear temperature gradient in top unit (°C/km)				
Linear temperature gradient in reservoir unit (°C/km)				
Linear temperature gradient in bottom unit (°C/km)				
Thermal expansion coefficient (1/°C)				
Thermal conductivity (W/m/°C)	2.9 Careful: Refers as "Wet heat conductivity" Unit is W/m/k			"see *Figure 17*" *Source: 1-s2.0-S0375650516300700-main.pdf (p.2)* See additional information in *Doddema (2012); 148285679.pdf (Appendix B)*
Specific heat capacity (J/kg/°C)	827 Careful: Unit is J/kg/k			"see *Figure 17*" *Source: 1-s2.0-S0375650516300700-main.pdf (p.2)* See additional information in *Doddema (2012); 148285679.pdf (Appendix B)*
Matrix density (kg/m³)	2500 - 2700 kg/m^3 2.67 kg/m^3 Careful: I think the unit is g/cm^3 2.705 – 2.682 g/cm^3 Careful: the unit is g/cm^3			"see *Figure 17*" *Source: 1-s2.0-S0375650516300700-main.pdf (p.2)* "see *Figure 22*" *Source: Doddema (2012); 148285679.pdf* "see *Figure 23*" *Source: tno report_ncp-2a_petrophysics_v150207.pdf*
Heat flow (mW/m²)				

Table 1
Initial state main inputs. Other porosity values for faults were also considered (5% and 15%) but proved to have little effect on the results, therefore a middle value of 10% was used throughout the analysis. Wet heat conductivity and specific heat values are based on data from several sources (Ondrak et al., 1998; Muntendam-Bos et al., 2008; Schön, 2011). Reservoir layer porosity and permeability data are detailed in Table 2.

Lithological group	Density (kg/m^3)	Porosity (%)	Permeability (horizontal) (mD)	Wet heat conductivity (W/m*$_K$)	Specific heat (J/kg*$_K$)
Zechstein salt (overburden)	2170	1	10^{-10}	3.5	1050
Rotliegend (reservoir)	2500–2700	variable	variable	2.9	827
Limburg (basement)	2900	1	10^{-2}	2.65	840
Faults	2800	10	variable	2.9	827

Figure 21 : (source: Daniilidis et al (2016)- 1-s2.0-S0375650516300700-main.pdf)

Table 3: Summary of rock properties.

		ZEZ2H	ZEZ2X	ROCLT	ROSLN	CARBF
Density	kg/m^3	2.11	2.83	2.72	2.67	2.63
Porosity	%	0	0	11	19	0
XY-Permeability	mD	0	0	50	250	0
Z-Permeability	mD	0	0	50	250	0
Wet heat conductivity	W/m/K	5.5	4.0	2.0	3.0	2.0
Specific heat	KJ/m^3/K	1050	830	870	980	870

Figure 22 : (source: Doddema (2012); 148285679.pdf)

Careful: I think the unit for density is g/cm^3

Table 4. Matrix density derived from measurement distributions for specific litho-stratigraphic units.

Litho-stratigraphic unit		Mean matrix density [g/cm^3]	Standard deviation [g/cm^3]
Schill Grund Formation	SLSS	2.710	0.016
Scruff Greensand Formation [1]	SLSG	2.634	0.026
Terschelling Formation (except SLCTO) [2]	SLCT	2.692	0.063
Oysterground Member	SLCTO	2.651	0.010
Friese Front Formation	SLCF	2.652	0.097
Solling Fat Sandstone member	RNSOF	2.540 [5]	- [5]
Detfurth Clay Member [3]	RBMDC	2.720	0.042
Lower Detfurth Sandstone Member	RBMDL	2.698	0.038
Volpriehausen Clay-Siltstone Member	RBMVC	2.720	0.042
Lower Volpriehausen Sandstone Member	RBMVL	2.645	0.040
Rogenstein Member	RBSHR	2.749	0.026
Ten Boer Member [4]	ROCLT	2.705	0.069
Upper Slochteren Member	ROSLU	2.705	0.069
Ameland Member [4]	ROCLA	2.705	0.069
Lower Slochteren Sandstone Member	ROSLL	2.682	0.014

[1] *Parameters derived from measurements on Scruff Spiculite Member (SLSGP)*

[2] *Parameters for sandstone units in SLCT derived from measurements on Terschelling Sandstone Member (SLCTS)*

[3] *Parameters derived from measurements on Volpriehausen Clay-Siltstone Member (RBMVC)*

[4] *Parameters derived from measurements on Upper Slochteren Member*

[5] *Applied mean matrix density determined based on best correlation (see text)*

Figure 23 : (source: Benedictus T (2007); *tno report_ncp-2a_petrophysics_v150207.pdf)*

For top layer: Zechstein Group

Property (unit)	Mean value	Min. value	Max. value	Source
Thermal expansion coefficient (1/°C)				
Thermal conductivity (W/m/°C)	3.5 Careful: Refers as "Wet heat conductivity" Unit is W/m/k			"see *Figure 17*" *Source: 1-s2.0-S0375650516300700-main.pdf (p.2)* See additional information in *Doddema (2012); 148285679.pdf (Appendix B)*
Specific heat capacity (J/kg/°C)	1050 Careful: Unit is J/kg/k			"see *Figure 17*" *Source: 1-s2.0-S0375650516300700-main.pdf (p.2)* See additional information in *Doddema (2012); 148285679.pdf (Appendix B)*

Matrix density (kg/m³)	2170 2.11 – 2.83 Careful: I think the unit is g/cm^3			"see *Figure 17*" *Source: 1-s2.0-S0375650516300700-main.pdf (p.2)* "see *Figure 22*" *Source: Doddema (2012); 148285679.pdf*
Heat flow (mW/m²)				

For bottom layer: Carboniferous (Limburg Group)

Property (unit)	Mean value	Min. value	Max. value	Source
Thermal expansion coefficient (1/°C)				
Thermal conductivity (W/m/°C)	2.65 Careful: Refers as "Wet heat conductivity" Unit is W/m/k			"see Figure 17" *Source: 1-s2.0-S0375650516300700-main.pdf (p.2)* See additional information in *Doddema (2012); 148285679.pdf (Appendix B)*
Specific heat capacity (J/kg/°C)	840 Careful: Unit is J/kg/k			"see Figure 17" *Source: 1-s2.0-S0375650516300700-main.pdf (p.2)* See additional information in *Doddema (2012); 148285679.pdf (Appendix B)*
Matrix density (kg/m³)	2900 kg/m^3 2.63 *kg/m^3* Careful: I think the unit is g/cm^3			"see *Figure 17*" *Source: 1-s2.0-S0375650516300700-main.pdf (p.2)* "see *Figure 22*" *Source: Doddema (2012); 148285679.pdf*
Heat flow (mW/m²)				

14. Fault property data

Property (unit)	Mean value	Min. value	Max. value	Source
Aperture at 0 MPa				

normal stress (m)				
Aperture at infinite normal stress (m)				
Dilation angle (°)				
Thickness (m)				
Porosity (-)	10 %			"see Figure 17" *Source: 1-s2.0-S0375650516300700-main.pdf (p.2)*
Friction coefficient (-)	0.23			"… the analysis show a better consistency with the recorded seismic events when using a cohesion of 7 MPa and a sliding friction angle of 13° (sliding friction coefficient = 0.23)" *Source: NAM (2015) Dynamic Geomechanical Modelling to Assess and Minimize the Risk for Fault Slip during Reservoir Depletion of the Groningen Field*
Cohesion (MPa)	7 MPa			
Young's modulus (GPa)				
Poisson's ratio (-)				

15.Stress and pressure data

For reservoir unit, adjacent formations (top and bottom unit), and above (may be the same in all units)

Property (unit)	Mean value	Min. value	Max. value	Source
Max. Hor. Stress direction (° from N)	N156°E - N160°E ± 10°			*source: NAM (2015) Dynamic Geomechanical Modelling to Assess and Minimize the Risk for Fault Slip during Reservoir Depletion of the Groningen Field)*
Pore pressure gradient above top unit (MPa/km)	Careful: Units are different in the Figure 24 graph			"see *Figure 24*" *(source: NAM (2015) Dynamic*
Pore pressure gradient in top unit (MPa/km)				
Pore pressure gradient in reservoir unit (MPa/km)				

Pore pressure gradient in bottom unit (MPa/km)				*Geomechanical Modelling to Assess and Minimize the Risk for Fault Slip during Reservoir Depletion of the Groningen Field)*
Min. hor. stress gradient above top unit (MPa/km)				
Min. hor. stress gradient in top unit (MPa/km)				
Min. hor. stress gradient in reservoir unit (MPa/km)	Sh = 1.54 and 1.67 SG (420-520 bars) at the top of the reservoir. Careful: This is not a gradient			*(source: NAM (2015) Dynamic Geomechanical Modelling to Assess and Minimize the Risk for Fault Slip during Reservoir Depletion of the Groningen Field)*
Min. hor. stress gradient in bottom unit (MPa/km)				
Max. hor. stress gradient above top unit (MPa/km)				
Max. hor. stress gradient in top unit (MPa/km)				
Max. hor. stress gradient in reservoir unit (MPa/km)	The predicted SH gradient in Groningen varies between 1.73 and 1.82 SG (500 – 560 bars) at the top of the Slochteren formation. Careful: This is not a gradient			*(source: NAM (2015) Dynamic Geomechanical Modelling to Assess and Minimize the Risk for Fault Slip during Reservoir Depletion of the Groningen Field)*
Max. hor. stress gradient in bottom unit (MPa/km)				
Vertical stress gradient above top unit (MPa/km)	Sv = Smax = between 2.19 and 2.35 SG at a reference level of 3000m TVDGL (ground level). This difference in vertical			"see *Figure 25*" *(source: NAM (2015) Neotectonic Stresses in the Permian Slochteren Formation of*
Vertical stress gradient in top unit (MPa/km)				
Vertical stress gradient in reservoir unit (MPa/km)				
Vertical stress gradient in bottom unit (MPa/km)				

	stress gradients is mainly caused by Zechstein salt thickness variations. Careful: Units are different in the Figure 24 graph			*the Groningen Field).*

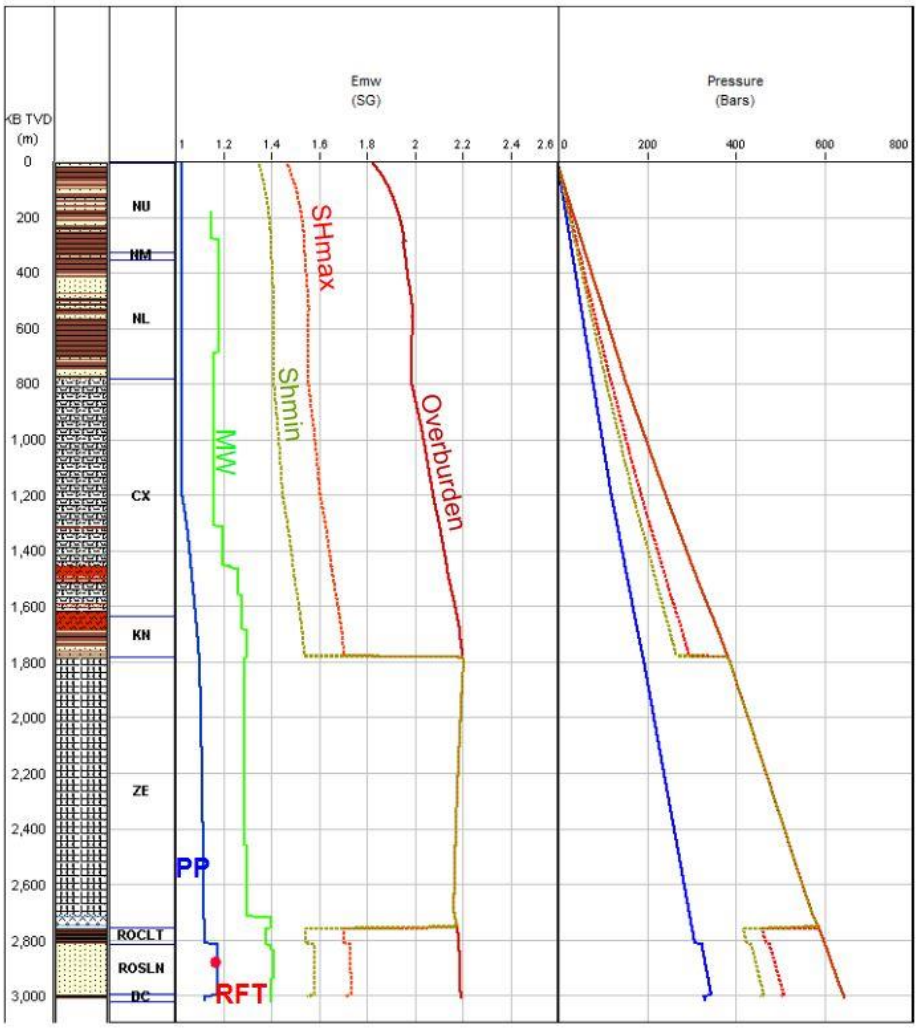

Figure 22. Summary of the principal stress magnitudes and the pore pressure as function of depth (example from well POS-1). S_v in dark red, S_{hmin} in dashed green, S_{Hmax} in dashed red and pore pressure in blue. Here is also displayed the MW used to drill this well (bright green) and the formation pressure measurements.

Figure 24: (source: NAM (2015) Dynamic Geomechanical Modelling to Assess and Minimize the Risk for Fault Slip during Reservoir Depletion of the Groningen Field)

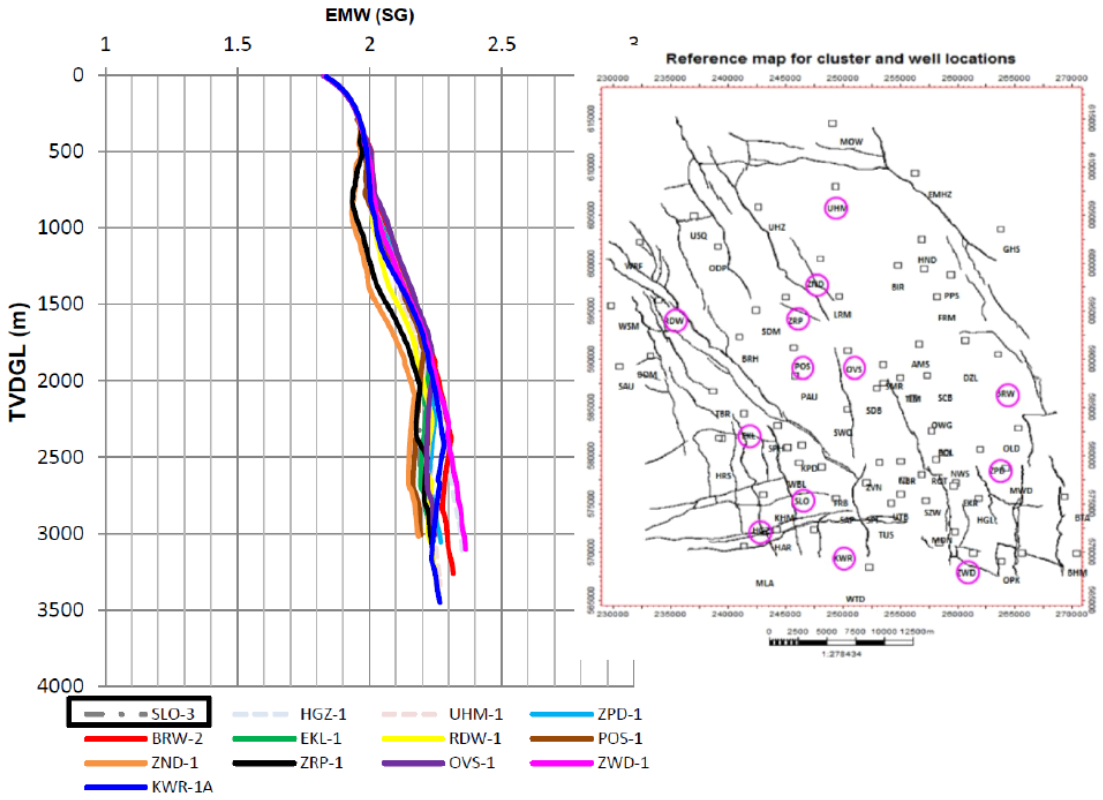

Figure 1 Vertical stress gradients (SG) for thirteen wells in the Groningen area. The overburden gradient varies from 2.19-2.35 SG at 3000m TVDGL (from Yan and Guises, 2013). To the right a map of the Groningen field showing the locations of the wells.

Figure 25 : (source: NAM (2015) Neotectonic Stresses in the Permian Slochteren Formation of the Groningen Field).

16. Reservoir fluid data

Reference temperature: 20°C

Property (unit)	Mean value	Min. value	Max. value	Source
Density (kg/m³)				
Viscosity (mPas)				
Thermal expansion coefficient (1/°C)				
Specific heat capacity (J/kg/°C)				
Thermal conductivity (W/m/°C)				
Salinity (g/L)				
Bulk modulus (GPa)				

Reference temperature: mean reservoir temperature : 90°C
(Middenmeer. *http://www.destress-h2020.eu/en/demonstration-sites/middenmeer/*
Heemskerk *https://wellengineeringpartners.com/geothermal-floricultura-heemskerk-doublet-delivery/*)

Property (unit)	Mean value	Min. value	Max. value	Source
Density (kg/m³)				
Viscosity (mPas)				
Thermal expansion coefficient (1/°C)				
Specific heat capacity (J/kg/°C)				
Thermal conductivity (W/m/°C)				
Salinity (g/L)	200 136			Middenmeer. *http://www.destress-h2020.eu/en/demonstration-sites/middenmeer/* The composition is believed to represent the composition of the brine in the Rotliegend. The equivalent NaCl concentration is 136 gram/litre, about 125,000 ppm. *Source: LEAN-D1.03-v2020.02.21-Reservoir-Characterization-Report-public.pdf (p. 29)*
Bulk modulus (GPa)				

17. Seismological data

Property (unit)	Mean value	Min. value	Max. value	Source
Criticality C(z) (Pa)				
Seismogenic index Σ (-)				
b-value (-)				

18. Operation/wellbore data

Property (unit)	Mean value	Min. value	Max. value	Source
Distance between injector and producer (m)				
Injection temperature (°C)				
Flow rate (l/s)				
Length of perforated/open interval (m)				
Inner diameter wellbore (m)				

Appendix C

Carboniferous Limestone

(Dinantian)

HELMHOLTZ CENTRE POTSDAM
GFZ GERMAN RESEARCH CENTRE FOR GEOSCIENCES

Dr. Hannes Hofmann

Section 4.8

Telegrafenberg

hannes.hofmann@gfz-potsdam.de

Telephone: +49 (0)331 288-28739

Potsdam, 07 September 2020

Data requirements for KEM-15 ("Cooling induced seismicity")

This document contains a list of data reqired to perform the numerical simulations of cooling induced seismicity using the Finite Element Code GOLEM. The model is based on the published and history matched GOLEM model of Groß Schönebeck Enhanced Geothermal System. Based on this model up to 5 generic and specific models will be built:

1 generic hydrothermal model (shallower, no stimulated fractures)
1 generic EGS model (deeper, with stimulated fractures)
1 specific hydrothermal reservoir above salt in the Netherlands
1 specific hydrothermal reservoir below salt in the Netherlands
1 specific deep EGS reservoir in the Netherlands

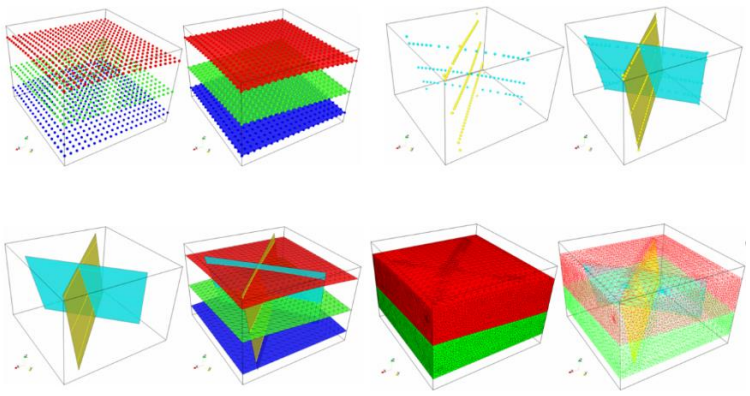

2500 Figure 26: Exemplary mesh generation of a generic 3D FEM model with 2 units and 2 faults.

For each of these models the parameter list below is required.

This document concerns the hydrothermal Ultra Deep reservoir in the Netherlands (EGS reservoir). The considered reservoir formation is the **Carboniferous Limestone Group** (of Dinantian age).

Stratigraphically, the Limburg Group (mostly composed by claystones) sits above the Carboniferous Limestone Group while the Devonian clastic sediments of the Banjaard Group sit below.

"The lowermost layer in the DGM-deep v4.0 model is the base of the Upper Carboniferous Limburg Group (DC), which corresponds to the top of the Lower Carboniferous. The carbonate rocks of the Lower Carboniferous are known, in the Netherlands, under various names: Dinantian, Carboniferous Limestone Group, Zeeland Formation, Kolenkalk, and sometimes "Kulm". The rocks are currently the target of geothermal exploration and production in the southern part of the Netherlands, where they are found at relatively shallow depths (~2 km). In a large part of the Netherlands, however, the rocks are buried very deep (~4-9 km), and therefore possibly interesting for Ultra Deep Geothermal ("UDG"). The rocks have a very low primary permeability but may exhibit karst and/or fault permeability." (*https://www.thermogis.nl/en/dinantian*).

"The carbonates often show low porosities and low permeabilities, but cross-cutting, high-angle fracture systems created some secondary porosity (Vandenberghe et al., 2000). In addition, the Upper Dinantian sediments were subjected to extensive karst processes creating cavernous karst systems with up to metre-scale cavities."
(*dinantian_carbonates_in_the_southern_netherlands_and_northern_belgium.pdf*)

"As the matrix permeability is very low, these systems rely on the presence of fractured, faulted and/or karstified limestones. The Dinantian Limestones are found in a large-scale anticlinal structure, situated in a horst block bounded by two major faults, the southwestern being the Tegelen fault. Within this horst block, the top of the Dinantian is partly eroded as a result of successive erosional events of which the significant ones are the Base Permian Unconformity and unconformities at the base Cretaceous and base North Sea Supergroup (Cenozoic)." (*Figure 27*)
(*Introduction_to_the_geothermal_play_and_reservoir_.pdf*)

Many of the parameter values added into the following tables refer to data collected from various documents and publications and do not apply to a single identified location.

Parameter values indicated in this document correspond to "geological" information (from well / care / sample analysis). Values derived from or used in modelling studies are not indicated in here.

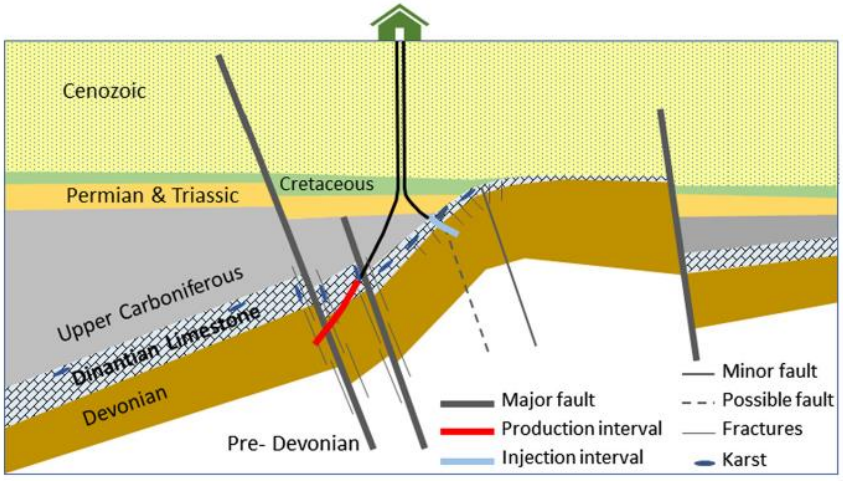

Figure 27 : Sketch of the subsurface architecture of the twogeothermal systems on the northern flank of the RoerValley Graben targeting the fractured Dinantian limestonesand Devonian sandstones. The sketch is modified after fig-ures in Californië Lipzig Gielen & VITO (2013). *Source: Introduction_to_the_geothermal_play_and_reservoir_.pdf*

19.Geological models (geometry)

For the specific reservoir models a GOCAD (*.gp) file of the reservoir geometry would be best. Alternatively, the individual faults, surfaces and well paths may be provided as point data (X, Y, Z). For the generic models the table below is enough.

Property (unit)	Mean value	Min. value	Max. value	Source
Reservoir unit top (m)	> 4 000 m if we consider an Ultra Deep Geothermal reservoir			See top Dinantian depth map *Source: top_dinantien_tvd_si_welltied.pdf* "In the larger part of the Netherlands, the Dinantian Limestone sequence is buried over 4 km. This would be ideal for producing heat in excess of 120°C for application in industrial processes." *Introduction_to_the_geothermal_play_and_reservoir_.pdf*
Reservoir unit thickness (m)				Base Dinantian is not known across the all Netherlands (*base_dinantien_tvd_si_welltied.pdf*) A thickness up to 768m for the Carboniferous Limestone Group is provided in *https://www.dinoloket.nl/en/stratigraphic-*

				nomenclature/carboniferous-limestone-group
Top layer thickness (m)				A thickness up to 895m for the Epen Formation (Geul Subgroup – Limburg Group) is provided in *https://www.dinoloket.nl/en/stratigraphic-nomenclature/epen-formation*
Bottom layer thickness (m)				A thickness up to 306m for the Banjaard group is provided in *https://www.dinoloket.nl/en/stratigraphic-nomenclature/banjaard-group*
# of fault sets	2			*Source:* *ndx_terheege.pdf*
Fault set strike (° from N)	N132°E and N164°E			
Fault set dip (° from hor.)	80°			
Fault set dip direction (° from N)	N042°E and N254°E			
Fault length (m)				
Fault spacing (m)				See description of fracture density and damaged zone in *Msc_thesis_Dominique_Reith_TU_Delft.pdf*
Units intersected by fault				

Information regarding fault strike and dip is also provided in:
Msc_thesis_Dominique_Reith_TU_Delft.pdf

"The FMI results of well CAL-GT-01S (ran in the top part of the Zeeland formation) shows that the bedding has a NS-strike and dips West with a mean dip angle of 22 degrees. The interpreted faults and micro-faults have a WNW-ESE to E-W strike and dip NE and SW with a mean dip angle of 87 degrees. …"

20. Rock mechanical data

For reservoir unit and adjacent formations (top and bottom layer)

Property (unit)	Mean value	Min. value	Max. value	Source
Young's modulus (GPa)				
Poisson's ratio (-)				
Tensile strength (MPa)				
UCS (MPa)				
Cohesion (MPa)				
Coefficient of internal friction (-)				
Coefficient of sliding friction (-)				
Matrix bulk modulus (GPa)				
Biot's coefficient (-)				

21. Hydraulic data

For reservoir unit and adjacent formations (top and bottom layer)

"The reservoir quality in the well (Luttelgeest-01) was poor. Matrix porosity is below 2%. This resulted in very low permeability. Only a few fracture zones were encountered on FMI. Two fracture zones correspond with the gamma ray peaks and indicate karstification horizons. The FMI indicated also a structural overprint with fractures in a N130-140 direction." *Source: 200906_EAGE_Luttelgeest_Abstract.txt*

Similar statement regarding the porosity and permeability of the potential reservoir in: *dinantian_carbonates_in_the_southern_netherlands_and_northern_belgium.pdf*. This paper also considers the karsts and fractured zones as preferential reservoir for the Dinantian.

Property (unit)	Mean value	Min. value	Max. value	Source
Horiz. Permeability (mD)		< 0.01 mD	2.2 mD	No mention if it is horizontal or vertical permeability!

				Source: dinantian_carbonates_in_the_southern_netherlands_and_northern_belgium_supp_materials.xlsx
Vert. Permeability (-)				
Porosity (-)	< 2%	0.4%	6% (26% in karst)	*Source: 200906_EAGE_Luttelgeest_Abstract.txt* *scan_dinantien_petrophysical_report_of_the_dinantian_carbonates_in_the_dutch_subsurface_0.pdf* *Source: dinantian_carbonates_in_the_southern_netherlands_and_northern_belgium_supp_materials.xlsx*

22.Thermal data

For reservoir unit and adjacent formations (top and bottom unit). Temperature gradient may be the same in all units.

Property (unit)	Mean value	Min. value	Max. value	Source
Linear temperature gradient above top unit (°C/km)	31 °C/km			"The average geothermal gradient in the Netherlands in 31°C/km with an average surface temperature of 10°C (Bonté et al, 2012). " *Introduction_to_the_geothermal_play_and_reservoir_.pdf* (p.7) See also, study specific to the Roer Valley Graben and West Netherlands Basin:
Linear temperature gradient in top unit (°C/km)				
Linear temperature gradient in reservoir unit (°C/km)				
Linear temperature gradient in bottom unit (°C/km)				

				Report_6425_Kennisagenda_V_2.1_def_FAULT.pdf
Thermal expansion coefficient (1/°C)				
Thermal conductivity (W/m/°C)				
Specific heat capacity (J/kg/°C)				
Matrix density (kg/m³)				
Heat flow (mW/m²)				

23. Fault property data

Leverink & Geel, 2019 estimate that analysis of Dutch Dinantian fracture suffers from a lack of data. This, combined with the varying nature of fracture characteristics, makes correlation between local and regional observations extremely difficult or even impossible.

Bibliographic data from several sources over the world have been compiled by Leverink & Geel (2019) to estimate the likely extreme values of fracture apertures in the Zeeland Formation.

Across the Belgian border, at the Balmatt project near Mol-Donk (MOL-GT wells), two FMI (Fullbore Formation MicroImager) interpretations independent from SCAN program were conducted for the Dinantian carbonates reservoir. Results from the MOL-GT wells which likely drilled through a fault have been presented at the European Geothermal Congress 2019 (Broothaers et al., 2019). An estimation of the aperture based on the FMI log provides an average value of 170 micrometre (pers. comm. In Leverink & Geel, 2019).

Information regarding faults may also be found in: *Msc_thesis_Dominique_Reith_TU_Delft.pdf*

Property (unit)	Mean value	Min. value	Max. value	Source
Aperture at 0 MPa normal stress (m)	170 µm (a)	3 µm (b)	2502 µm (b)	(a) Broothaers et al., 2019 (b) Leverink & Geel (2019) p.21 *NLOG_GS_PUB_1519_SCAN_Fracture_Characterization_of_the_Dinantian_Carbonates_in_the_Dutch_Subsurface.pdf*
Aperture at infinite normal stress (m)				
Dilation angle (°)				

Thickness (m)				
Porosity (-)				
Friction coefficient (-)				
Cohesion (MPa)				
Young's modulus (GPa)				
Poisson's ratio (-)				

24.Stress and pressure data

For reservoir unit, adjacent formations (top and bottom unit), and above (may be the same in all units)

Information regarding pressure distribution and fluid flow for both the Dinantian and the overlying Limburg Group are provided in: *"Pressure and fluid dynamic characterisation of the Dutch subsurface" by Verweij et al. (2012) (pdf file: Verweij-NJG-91-4-4_2012.pdf)*

Property (unit)	Mean value	Min. value	Max. value	Source
Max. Hor. Stress direction (° from N)	See Figure 2			"From the limited data that is available, it appears that horizontal stress azimuths and gradients obtained in overlying formations nearby can be used to estimate the state of stress in the Dinantian….. This hypothesis may not hold in areas where Namurian shales cover the Dinantian carbonates." *Source: scan_dinantian_stress_field_characterization_dinantian_carbonates_report.pdf*
Pore pressure gradient above top unit (MPa/km)				See informations in : *Verweij-NJG-91-4-4_2012.pdf*
Pore pressure gradient in top unit (MPa/km)				
Pore pressure gradient in				

reservoir unit (MPa/km)				
Pore pressure gradient in bottom unit (MPa/km)				No data are provided below the Dinantian reservoir
Min. hor. stress gradient above top unit (MPa/km)				
Min. hor. stress gradient in top unit (MPa/km)				
Min. hor. stress gradient in reservoir unit (MPa/km)				"From the limited data that is available, it appears that horizontal stress azimuths and gradients obtained in overlying formations nearby can be used to estimate the state of stress in the Dinantian….. This hypothesis may not hold in areas where Namurian shales cover the Dinantian carbonates." *Source: scan_dinantian_stress_field_ characterization_dinantian_ carbonates_report.pdf*
Min. hor. stress gradient in bottom unit (MPa/km)				No data are provided below the Dinantian reservoir
Max. hor. stress gradient above top unit (MPa/km)				
Max. hor. stress gradient in top unit (MPa/km)				
Max. hor. stress gradient in reservoir unit (MPa/km)				"From the limited data that is available, it appears that horizontal stress azimuths and gradients obtained in overlying formations nearby can be used to estimate the state of stress in the Dinantian….. This hypothesis may not hold in areas where Namurian shales cover the Dinantian carbonates." *Source: scan_dinantian_stress_field_*

				characterization_dinantian_ carbonates_report.pdf
Max. hor. stress gradient in bottom unit (MPa/km)				No data are provided below the Dinantian reservoir
Vertical stress gradient above top unit (MPa/km)				
Vertical stress gradient in top unit (MPa/km)				
Vertical stress gradient in reservoir unit (MPa/km)				
Vertical stress gradient in bottom unit (MPa/km)				

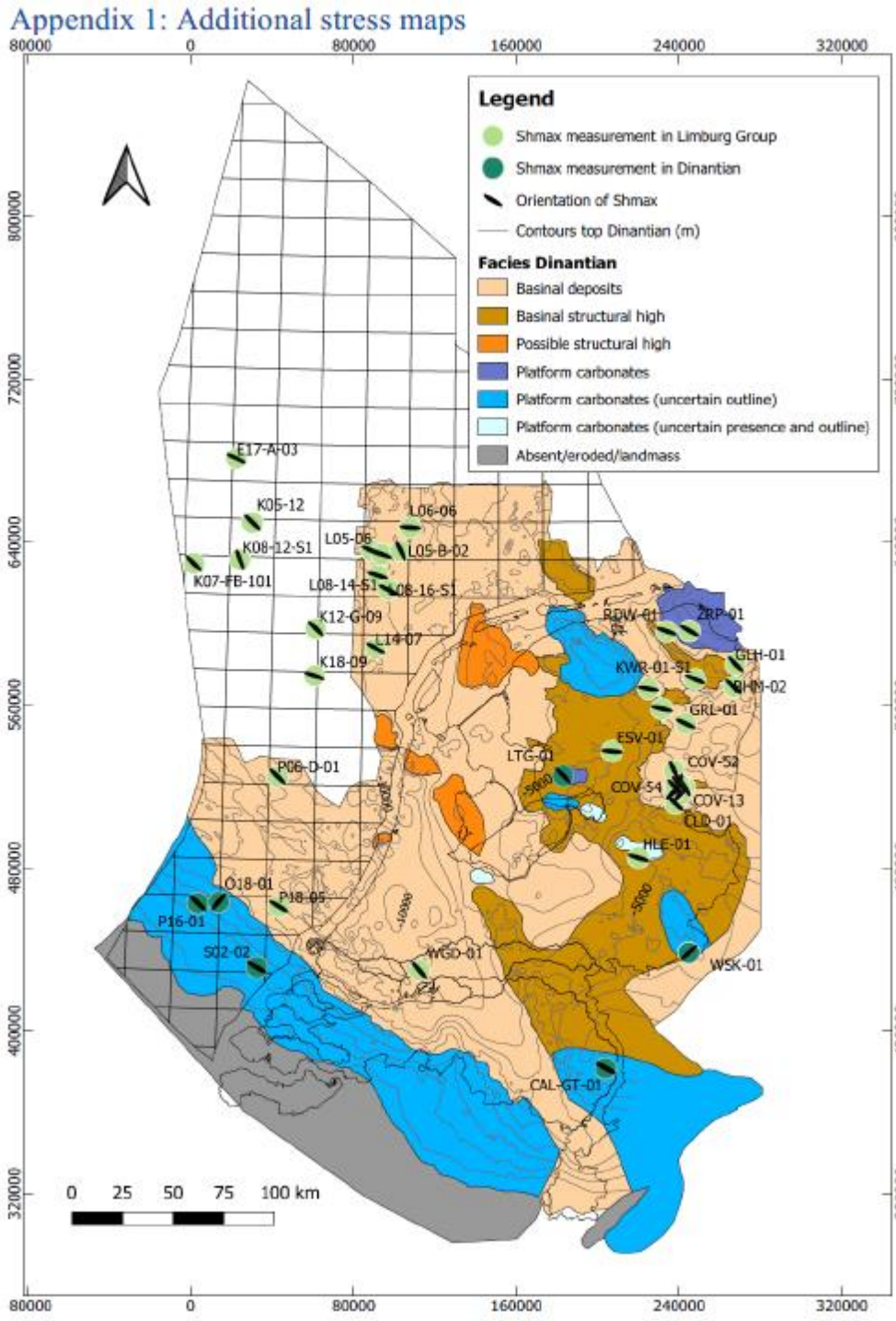

Figure 13: Combination of all S_{Hmax} orientation data in both the Limburg Group (Mechelse, 2017) and the Dinantian (this work). Dinantian facies map (Seq 2 & 3) from Mozafari et al, 2019

Figure 28 : SHmax orientation map for Limburg Group and Dinantian

source: scan_dinantian_stress_field_characterization_dinantian_carbonates_report.pdf

25.Reservoir fluid data

Reference temperature: 20°C

Property (unit)	Mean value	Min. value	Max. value	Source
Density (kg/m³)				
Viscosity (mPas)				
Thermal expansion coefficient (1/°C)				
Specific heat capacity (J/kg/°C)				
Thermal conductivity (W/m/°C)				
Salinity (g/L)				
Bulk modulus (GPa)				

Reference temperature: mean reservoir temperature

Property (unit)	Mean value	Min. value	Max. value	Source
Density (kg/m³)				
Viscosity (mPas)				
Thermal expansion coefficient (1/°C)				
Specific heat capacity (J/kg/°C)				
Thermal conductivity (W/m/°C)				
Salinity (g/L)				
Bulk modulus (GPa)				

26.Seismological data

Property (unit)	Mean value	Min. value	Max. value	Source
Criticality C(z) (Pa)				
Seismogenic index Σ (-)				
b-value (-)				

27.Operation/wellbore data

Property (unit)	Mean value	Min. value	Max. value	Source
Distance between injector and producer (m)				
Injection temperature (°C)				
Flow rate (l/s)				
Length of perforated/open interval (m)				
Inner diameter wellbore (m)				